

Synthesis and NMR-Driven Conformational Analysis of Taxol Analogues Conformationally Constrained on the C13 Side Chain

Luciano Barboni* and Catia Lambertucci

Dipartimento di Scienze Chimiche, Università di Camerino Via S. Agostino 1, I-62032 Camerino (MC), Italy

Giovanni Appendino*

DiSCAFF, Università del Piemonte Orientale Viale Ferrucci 33, 28100 Novara, Italy

David G. Vander Velde† and Richard H. Himes‡

Departments of Medicinal Chemistry and Molecular Biosciences, University of Kansas, Lawrence, Kansas 66045

Ezio Bombardelli

Indena S.p.A., Viale Ortles 12, 20139 Milano, Italy

Minmin Wang and James P. Snyder*

Department of Chemistry, Emory University, Atlanta, Georgia 30322

Received October 24, 2000

Analogues of Taxol (paclitaxel) with the side chain conformationally restricted by insertion of a carbon linker between the 2'-carbon and the *ortho*-position of the 3'-phenyl ring were synthesized. Biological evaluation of these new taxoids showed that activity was dependent on the length of the linker and the configuration at C2' and C3'. Two analogues in the homo series, **9a** and **24a**, showed tubulin binding and cytotoxicity comparable to that of Taxol. NAMFIS (NMR analysis of molecular flexibility in solution) deconvolution of the averaged 2-D NMR spectra for **9a** yields seven conformations. Within the latter set, the hydrophobically collapsed "nonpolar" and "polar" classes are represented by one conformation each with predicted populations of 12–15%. The five remaining conformers, however, are extended, two of which correspond to the T-conformation (47% of the total population). The latter superimpose well with the recently proposed T-Taxol binding conformer in β -tubulin. The results provide evidence for the existence of two previously unrecognized structural features that support Taxol-like activity: (1) a reduced torsion angle between C2' and C3' and (2) an orthogonal arrangement of the mean plane through C1', C2' and the 2'-hydroxyl and the 3'-phenyl plane, the latter ring bisected by the former plane. By contrast, epimerization at 2',3' and homologation of the tether to CH₂–CH₂ were both detrimental for activity. The decreased activity of these analogues is apparently due to configurational and steric factors, respectively.

Introduction

The discovery that Taxol (paclitaxel, **1a**) binds to tubulin promoting its aggregation in microtubules and the disclosure of its potential clinical activity in various forms of cancer have put this complex diterpenoid at the center of intense multidisciplinary attention and extraordinary media attention.¹ Within the chemical arena, the search for improved analogues has generated an impressive body of structure–activity data (SAR).² The amino acid side chain and, to a lesser extent, also the terpenoid core of the natural product turned out to be amenable to modification for the synthesis of analogues. Early studies led to the discovery of Taxotere

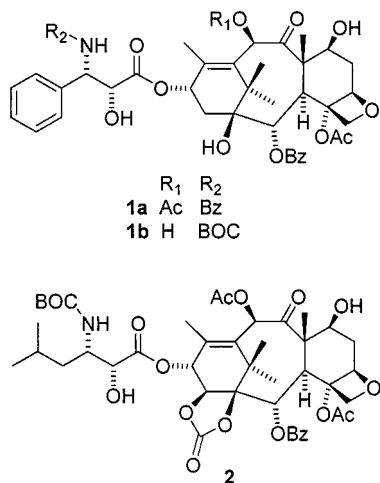
(docetaxel, **1b**),³ a clinically useful compound with a better solubility and a higher in vitro potency compared to Taxol. More recent investigations have focused on analogues active on MDR (multi-drug-resistant) cells, easier to administer, and endowed with a better profile of side effects⁴ as exemplified by the orally active taxoid IDN 5109 (**2**).⁵

The discovery of Taxol-mimicking compounds which structurally deviate from the taxoid platform and superficially do not resemble each other has proven of great significance in the field,⁶ suggesting the existence of a shared structural core among the various tubulin stabilizers. The structural elements underlying the occupation of an identical binding site are not obvious, and the pharmacophore models which have emerged from the vast body of information available are contrasting and focus on different functionalities.⁷ The problem is complicated by the fact that an endogenous ligand has not yet been identified, and therefore, it is not known what endogenous ligand, if any, the various

* To whom correspondence should be addressed. Luciano Barboni: phone, +39 0737 402240; fax, +39 0737 637345; e-mail, barboni@camserv.unicam.it. Giovanni Appendino: phone, +39 011 670 7684; fax, +39 011 670 7687; e-mail, appendin@pharm.unito.it. James P. Snyder: phone, 404-727-2415; fax, 404-727-6586; e-mail, snyder@euch4e.chem.emory.edu.

† Department of Medicinal Chemistry, University of Kansas.

‡ Department of Molecular Biosciences, University of Kansas.

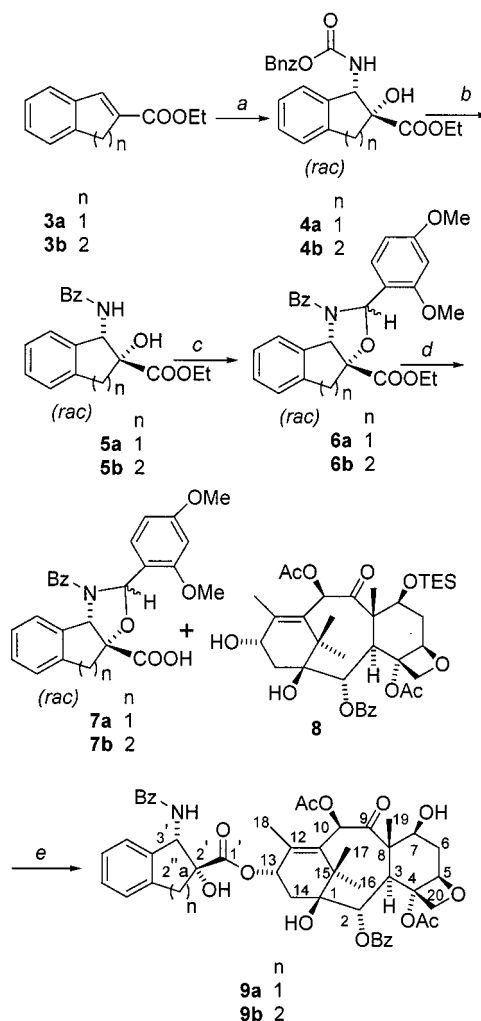


tubulin stabilizers are supposed to mimic. The discovery of a second receptor for Taxol⁸ has added a further layer of complexity to our understanding of the structural requirements for cytotoxic activity, since little is known about the interaction of the biological analogues of Taxol with this receptor. A further complicating factor is the poor correlation between tubulin binding and cytotoxicity that has sometimes been observed for taxoids.⁹

At the core of the ambiguity in the definition of a taxoid pharmacophore is the issue of the active conformation of the natural product, and a significant amount of research has focused on the alleviation of this problem. The baccatin core of Taxol is conformationally rigid, but the side chains are not, and the presence of at least seven easily rotated single bonds within these moieties translates into a palette of three basic types of conformations: two globular and an extended one.¹⁰ The two globular conformers are characterized by a clustering of the lipophilic groups on the amino acid side chain and the terpenoid core and are often referred to as the nonpolar and the polar forms, since first detected in CDCl₃ and water–DMSO, respectively.^{10c} The importance of the extended conformational type devoid of intramolecular hydrophobic interactions was recognized only recently in the deconvolution of the averaged NMR spectra of Taxol in chloroform^{10h} and at the β -tubulin binding site.^{10i,11}

In an ingenious approach to the taxane pharmacophore, Ojima reported analogues where the amino acid chain and the lipophilic ester group at C2 are merged into a macrocyclic diester.^{7c,12} The activity of some of these compounds is a highly significant finding, but its translation into conformational terms is complicated by the flexibility of the tether. To simplify the recognition of the still elusive active conformation of anticancer taxoids, we planned the synthesis of constrained analogues where rotation around the bonds C2'–C3' and C3'–phenyl, both pivotal event in the dynamic averaging observed in solution, is blocked or reduced by a short covalent tether between the 2'-carbon and the *ortho*-position of the 3'-phenyl ring.¹³ These compounds retain the rich functionality of Taxol but only part of its conformational complexity. Since the introduction of a methyl on the 2'-position of Taxol and Taxotere is well-tolerated in terms of activity,¹⁴ the biological evaluation of these tethered analogues should help define a more

Scheme 1^a

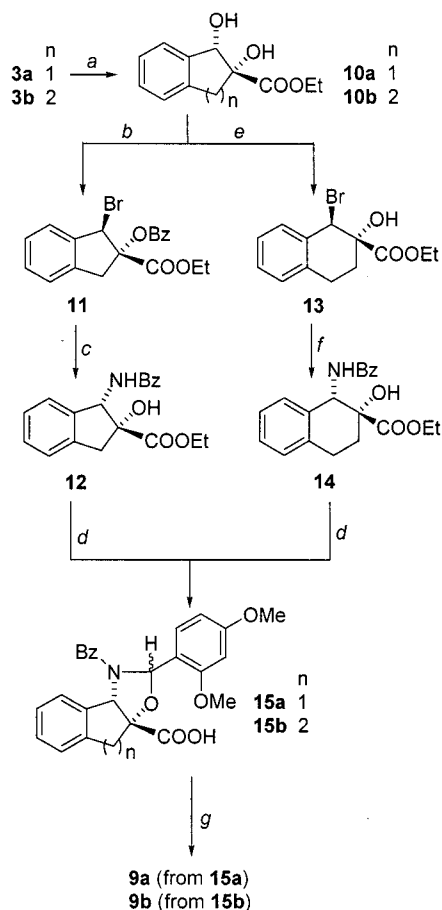


^a (a) BnZOCONH₂, NaOH, *t*-BuOCl, (DHQ)₂PHAL, K₂OsO₂(OH)₄, *n*-PrOH, H₂O (45% for **4a**, 33% for **4b**); (b) i. HCOONH₄, Pd(C), AcOH, ii. PhCOCl, NaHCO₃, CH₂Cl₂–H₂O (68% for **5a**, 70% for **5b**); (c) 2,4-dimethoxybenzaldehyde dimethylacetal, PPTS, toluene, Δ ; (d) K₂CO₃, MeOH–H₂O; (e) i. DCC, DMAP, toluene, rt, ii. 0.1 M HCl in MeOH (29% from **5a** for **9a**, 24% from **5b** for **9b**).

precise pharmacophore model for the interaction of anticancer taxoids and tubulin.

Chemistry

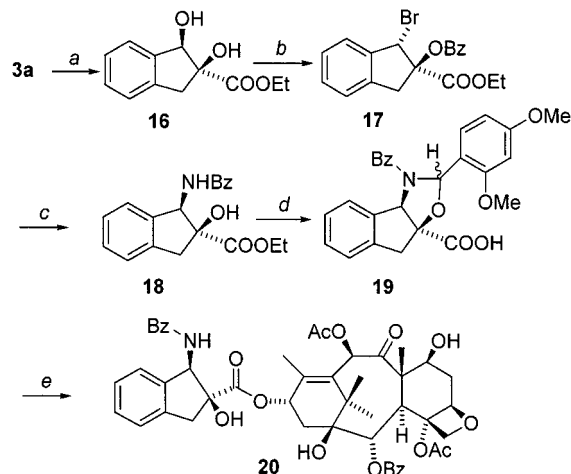
Several methods have been developed to convert cinnamic acid derivatives to the side chain of anticancer taxoids,¹⁵ and the tethered cinnamates **3a,b** were identified as logical precursors of the side chains needed for the synthesis of the target taxoids. The asymmetric aminohydroxylation (AA)¹⁶ of both esters (Scheme 1) occurred with remarkable regioselectivity but gave essentially racemic amino alcohols, as evidenced by an HPLC analysis of the corresponding *N*-decarbamoyle-*N*-menthylcarbonates¹⁷ (ee ca. 0 for **4a** and <10 for **4b**). Reductive decarbamylation of the amino alcohols **4a,b**, followed by remodeling of the substitution pattern of the heteroatoms via *N*-acylation and amination formation with 2,4-dimethoxybenzaldehyde dimethylacetal,¹⁸ eventually gave the oxazolidinones **6a,b**. Saponification to the corresponding acids **7a,b** and coupling with 7-OTES-(=triethylsilyl)-baccatin III (**8**) using the DCC–DMAP protocol completed the synthesis. Kinetic resolution took

Scheme 2^a

^a (a) ADmix- α , *t*-BuOH–H₂O 1:1 (65% for **10a**, 77% for **10b**); (b) i. trimethyl orthobenzoate, PTSA, ii. AcBr (72%); (c) i. NaN₃, DMF, 45 °C, ii. H₂, Pd/C, EtOH (overall 21%); (d) 2,4-dimethoxybenzaldehyde dimethylacetal, PPTS, toluene, Δ ; (e) i. SOCl₂, pyridine, CH₂Cl₂, ii. NaIO₄, RuCl₃, MeCN, iii. (*n*-Bu)₄NBr, Me₂CO–H₂O, H₂SO₄ (20% from **10b**); (f) i. NaN₃, DMF, ii. H₂, Pd/C, EtOAc, iii. BzCl, NaHCO₃, CH₂Cl₂–H₂O (overall 87%); (g) i. **8**, DCC, DMAP, toluene, rt, ii. 0.1 M HCl in MeOH (35% from **12** for **9a**, 29% from **14** for **9b**).

place in the esterification of the 13-hydroxyl affording, after deprotection, the diastereomerically pure taxoids **9a,b**. Kinetic resolution in the esterification of the 13-hydroxyl of protected baccatins has been reported with both acids and β -lactams, affording taxoids with the natural 2*R*,3*S* configuration.¹⁹ However, unambiguous evidence for this configuration could not be obtained by NMR analysis of **9a,b**. Since the activity of 2'-substituted taxoids is critically dependent on the configuration at C2' and C3',^{14a} and all reported cases of kinetic resolution were observed with acylating reagents lacking an α -alkyl substituent,¹⁹ the configurational assignment of **9a,b** was secured by an independent asymmetric synthesis.

To this purpose, we capitalized on an asymmetric dihydroxylation strategy, since the vast body of data available on the reaction of substituted cinnamates provides a straightforward configurational assignment.²⁰ Thus, treatment of **3a,b** with the ADmix- α afforded the diols **10a,b** (Scheme 2) with satisfactory enantioselectivity (ca. 92% ee, based on HPLC analysis of the diastereomeric menthylcarbonates¹⁷). A straightforward oxygen-to-nitrogen substitution via an orthoester-mediated double inversion protocol²¹ was employed

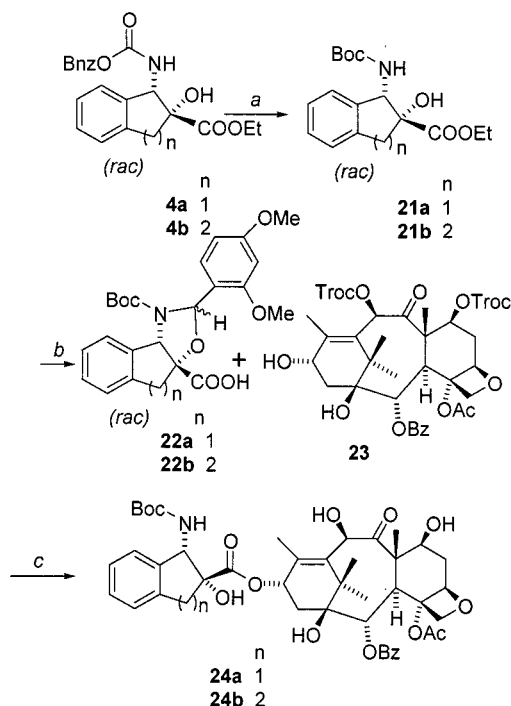
Scheme 3^a

^a (a) ADmix- β , *t*-BuOH–H₂O 1:1 (63%); (b) i. trimethyl orthobenzoate, PTSA, ii. AcBr (70%); (c) i. NaN₃, DMF, 45 °C, ii. H₂, Pd/C, EtOH (overall 25%); (d) 2,4-dimethoxybenzaldehyde dimethylacetal, PPTS, toluene; (e) i. **8**, DCC, DMAP, toluene, 70 °C, ii. 0.1 M HCl in MeOH (11% from **18**).

for the synthesis of the side chain of the homo-taxane **9a**. To this purpose, **10a** was sequentially treated with phenyl orthoformate and acetyl bromide, cleanly affording the *O*-benzoylated bromide **11**, next treated with NaN₃ in DMF. Azide to amine reduction with concomitant oxygen to nitrogen acyl rearrangement, followed by oxazolidine formation and saponification, eventually afforded the scalemic side chain precursor **15a**. Coupling with 7-TES-baccatin III (**8**) and deprotection gave a compound identical to the one obtained from the racemic acid **7a**. Unexpectedly, the orthoester-mediated double-inversion protocol²¹ failed with diol **10b**, but the required bromide could be obtained via a sulfate-mediated double-inversion strategy.²² Thus, treatment of **10b** with thionyl chloride gave a sulfite, which was oxidized to the corresponding sulfate and nucleophilically opened with tetrabutylammonium bromide to afford the *trans*-bromohydrin **13**. The synthesis was completed uneventfully as described for **11**, providing the scalemic acid **14**. Also in this case, protection as a 2,4-dimethoxybenzyl acetal and coupling with 7-TES-baccatin III (**8**) afforded, after deprotection, a compound identical to the one obtained from the racemic acid.

With the configurational assignment of **9a,b** secured, we went on to prepare the corresponding Taxotere analogues and modify the active (see *infra*) 2',2'-methylene analogue **9a** by changes in the configuration at C2', C3'. The 2'*S*,3'*R*-acid **19** was prepared using the same sequence used for the synthesis of its enantiomer **9a**, but employing the ADmix- β for the AD step (Scheme 3). The observation that the acid **19** and 7-TES-baccatin III (**8**) were essentially unreactive under standard coupling conditions confirmed that they constitute, in stereochemical term, a mismatched pair. Nevertheless, under forcing conditions, coupling could be achieved, albeit in poor yield, affording the taxoid **20**.

The *N*-debenzoyl-*N*-Boc(= *tert*-butoxycarbonyl) acids **22a,b** were prepared using the sequence employed for the synthesis of their racemic *N*-benzoyl analogues **7a,b** but replacing benzoyl chloride with Boc-anhydride in the acylation step (Scheme 4). Once more, complete kinetic resolution was observed in the coupling with 7-

Scheme 4^a

^a (a) i. HCOONH₄, Pd(C), AcOH, ii. (Boc)₂O, NaHCO₃, CH₂Cl₂-H₂O (68% for **21a**, 66% for **21b**); (b) i. 2,4-dimethoxybenzaldehyde dimethylacetal, PPTS, toluene, Δ (80%), ii. K₂CO₃, MeOH-H₂O (80% from **21a** for **22a**, 78% from **21b** for **22b**); (c) i. DCC, DMAP, toluene, rt, ii. 0.1 M HCl in MeOH, iii. Zn, AcOH, MeOH (17% for **24a**, 4% for **24b**).

Table 1. Biological Evaluation of the 2',2''-Conformationally Constrained Taxoids^a

compd	tubulin binding (ED ₅₀ /ED ₅₀ (Taxol))	cytotoxicity, MCF7 cells (ED ₅₀ /ED ₅₀ (Taxol))
9a	4	9
9b	42	333
20	inactive	1604
24a	7	2
24b	30	239

^a The ED₅₀ of Taxol in the tubulin assembly assay was 0.2 to 0.4 μM. The ED₅₀ of Taxol in the cytotoxicity assay was 2 to 4 nM.

10-di-Troc(=trichloroethoxycarbonyl)-10-deacetyl-baccatin III (**23**), affording the diastereomerically pure Taxotere analogues **24a,b**.

Results and Discussion

Biological Evaluation. The series of five 2',2''-alkylidene constrained taxoids (**9a,b**, **20**, **24a,b**) was tested for tubulin binding and cytotoxicity. Taxol was used as a reference compound for both assays, and the results are presented in Table 1. Introduction of a methylene bridge between the 2'-carbon and the *ortho*-position of the 3'-phenyl gave analogues of Taxol and Taxotere retaining strong tubulin binding and cytotoxicity (**9a** and **24a**, respectively). Conversely, replacement of the methylene link with an ethylidene, as in **9b** and **24b**, led to a dramatic decrease of activity in both assays, while epimerization of **9a** at C2', C3' afforded a practically inactive compound (**20**). A good correlation between tubulin binding and cytotoxicity was observed for all compounds.

Conformational Considerations. The activity of the C2', C2'' conformationally constrained analogues of

Table 2. Mole Fractions (MF) and Selected Geometric Features for the Seven MM3* Optimized Conformations of **9a** Derived from NAMFIS Analysis in DMSO-*d*₆ Compared with Taxol and Taxotere Conformers.

compd	MF (%)	selected dihedral angles (deg)		
		X-2'-3'-Ph ^a	1'-2'-3'-Ph	O=1'-2'-OH
9a1	26	-37	-158	36
9a2	21	33	-85	27
9a3	15 ^b	-35	-156	38
9a4	15 ^b	-35	-157	37
9a5	12	34	-83	57
9a6	10	-37	-155	177
9a7	2	-34	-157	36
25a^c		66	-58	41
25b^d		60	-65	93
26^e		-61	-179	-2
27^f		-53	-170	14

^a For **9a1**-**9a7**, X = CH₂; for **25**-**27**, X = H. ^b Differences in other dihedral angles distinguish these conformations; e.g. C12-C13-O(ether)-C1' and O(ether)-C1'-C2'-C3'. ^c The "polar" form of Taxol, ref 23. ^d The extended form of Taxol, ref 23. ^e Taxotere, ref 22. ^f T-Taxol, ref 10i.

Taxol is critically dependent on the length of the tether and the configuration at C2' and C3'. The excellent antitumor activity and tubulin affinity of 2'-methyl taxoids were fundamentally maintained in the methylene-linked compounds **9a** and **24a**, showing that tethering of the extra C2' methyl to the *ortho*-carbon of the 3'-phenyl is compatible with tubulin binding and cytotoxicity. A conformational hallmark of these compounds is the perpendicular location of the mean plane through C1', C2' and the 2'-hydroxyl and the 3'-phenyl plane, the latter ring bisected by the former plane. This is an unusual arrangement not found in other taxoids. In the solid state, the same elements of Taxotere,²³ the two conformations of Taxol,²⁴ and the amino acid side chain of Taxol²⁵ adopt alternative orientations. Furthermore, the modest puckering of cyclopentene derivatives means that in **9a** and **24a** the CH₂(corresponding to H2' of Taxol)-C2'-C3'-Ph torsion angle has values restricted to around +30 and -30° (Table 2). This is at the border between the *gauche* and eclipsed domains and significantly lower than those detected in the X-ray analysis of conformationally unconstrained anticancer taxoids (Taxol 60° and 66° (polar),²⁴ Taxotere -61°²³). The finding that these changes are well-tolerated in terms of activity suggests that there may be a taxoid family of conformers supporting a narrow window of H-C2'-C3'-Ph dihedral angles that are ideal for tubulin binding.

The dramatic loss of activity observed upon isomerization of **9a** at C2' and C3' closely parallels the results observed in 2'-methyl substituted taxoids and is in sharp contrast to what is observed in Taxol and Taxotere, whose 2'*S*,3'*R* diastereomers retain a noteworthy activity in both cytotoxicity and binding assays.²⁶ Apparently, the presence of an acyclic alkyl substituent at C2' renders the compounds unable to compensate in conformational terms for diastereomeric changes in the side chain. Similarly, the sharp decrease of activity observed in the ethylidene-linked compounds **9b** and **24b** is striking. Ring puckering is expected to increase from indans to their corresponding tetrahydronaphthalene derivatives, translating into higher conformational barriers for **9b** and **24b**.

Steric factors might also play a role, preventing C2' substituents larger than a methyl group from being

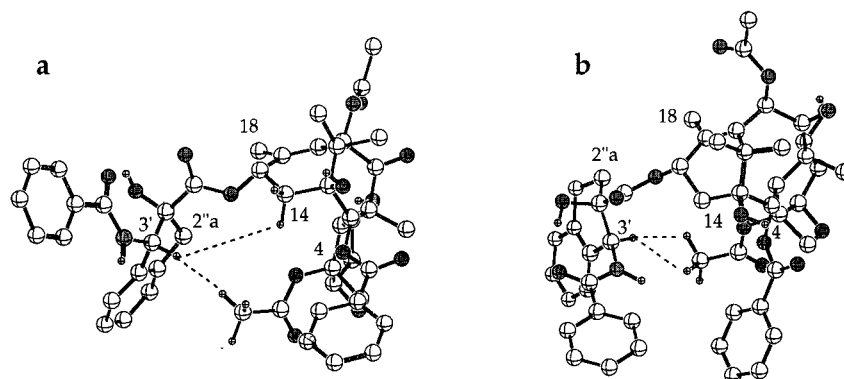


Figure 1. Lowest energy conformations of **9a,b** as derived by NAMFIS analysis with the diterpenoid cores depicted in a similar orientation (a, **9a1**; b, **9b1**). The dotted lines indicate prominent NOE cross-peaks between C3'-H and the cross-cavity protons of the C4-OAc methyl and C14-H.

accommodated in the binding groove of tubulin which recognizes the side chain of taxoids. Docking of **9a,b** into refined models of β -tubulin is supportive of this postulate.²⁷

The convex shape of the baccatin core makes it possible for α -oriented ester groups at C2, C4, and C13 to engage in hydrophobic interactions.¹⁰ In Taxol, the flexibility of these side chains translates into a palette of different conformations, two extremes being the so-called "nonpolar" and "polar" conformations, where the C2 benzoate phenyl ring clusters with the *N*-acyl group and the 3'-phenyl of the amino acid side chain, respectively.¹⁰ These conformations are exemplified by the X-ray geometries of Taxol²⁴ and Taxotere,²³ but rapid equilibration occurs in solution resulting in several families of rotamers. In chloroform, a bias toward "nonpolar" forms with small H2'-H3' torsion angles is observed,^{10h} while the contribution of the "polar" form with a large H2'-H3' torsion angle is increased in water-DMSO.¹⁰ One of the indices of these changes is rotation around the C2'-C3' bond. Since the 2'-2'' tether limits rotation, the conformations of **9a,b**, **20**, and **24a,b** might differ substantially from Taxol. Thus, the side chain conformational behavior of these compounds in solution was investigated by combining NOESY and ROESY NMR experiments with NAMFIS analysis.^{28a,b}

2-D NOEs and NAMFIS Analysis. Compound **9a**, incorporating a five-membered ring between C2' and the *ortho*-position of the C3' phenyl ring, presented 14 cross-peaks in its 2-D NOESY NMR spectrum in DMSO-*d*₆. When the peak volumes were referenced to the conformationally immobile H7-H10 distance of 2.40 Å, 14 averaged intramolecular distances could be calculated (see Experimental Section). To perform a conformational deconvolution with the NAMFIS technique, structure **9a** was subjected to a Monte Carlo conformational search with the MM3*/GBSA/H₂O force field.^{29a-c} The resulting 1121 optimized conformers were combined with the NOE-derived distances by means of the NAMFIS least-squares fitting procedure to give seven conformations, **9a1-9a7**, with predicted solution populations ranging from 2-26%.

The structure predicted to be most populated, **9a1** (Table 2), is pictured in Figure 1. The C13 side chain is in an extended conformation; neither terminal phenyl ring "collapsed" with the C2 benzoyl phenyl. A noteworthy feature of the structure is the location of the 4-OAc methyl group above the face of the indan aro-

matic ring consistent with an upfield π -electron-induced chemical shift of the acetate methyl and pronounced NOEs between these groups.³⁰ Relative to Taxol, the 4-acetyl signal in **9a** is shifted upfield δ 0.51 in CDCl₃ and δ 0.38 in DMSO. In 3'-alkyl analogues,³¹ where π -aromatic effects are absent, and in 2'-alkyl analogues, where altered side chain conformations appear,^{14a} the 4-acetyl is shifted downfield relative to Taxol. The face-on approach of the 4-acetate to the bicyclic system can be achieved in only one possible orientation, namely with the C3' hydrogen directed inward with respect to the concave shape of the diterpenoid core. At the same time, the C13-O and C1'-C2' bonds adopt torsional angles that bring the indan aromatic ring over the acetate methyl group. In **9a**, strong to medium NOEs are observed between H2''a and the 18-methyl and between H3' and the 4-OAc methyl, as well as between H3' and H14 α . Structure **9a1** fulfills the first two NOE observations with four proton-proton distances within the range 2.9-3.9 Å and two H...H separations of 2.4-3.0 Å, respectively. Accordingly, as pictured in Figure 1, the 2''a hydrogens are *syn* to Me-18 and the C3' proton is located within the concave region of the molecule rather than directed outward from the convex surface. However, it should be remembered that the NOEs are averaged across all seven conformations. Thus, **9a3** and **9a4**, assigned populations of 15% each (Table 2), contribute to the H3'-H14 α NOE cross-peaks with distances of 3.6 and 3.1 Å, respectively. Both likewise exhibit a face-on relationship between 4-OAc methyl and the indan aromatic ring.

There are three additional distinctive features of the **9a** NAMFIS conformations. First, all known families of conformers are represented. Five forms, **9a1**, **9a2**, **9a3**, **9a6** and **9a7**, fall into a group characterized by the lack of hydrophobic collapse between C2 and C3' hydrophobes. Structure **9a4** (15%) resides in the "nonpolar" category as a result of aromatic collapse between C3'-NHCO-Ph and C2-OCO-Ph. By contrast, **9a5** (12%) is of the "polar" type exhibiting a tight cluster among the C2 phenyl, the indan aromatic ring, and the C4 OAc methyl groups. Second, the indan five-membered ring in **9a** is capable of puckering to give two envelope conformations, A and B (Figure 2). Conformers **9a2** and **9a5** belong in the A class with the benzamidophenyl moiety in a pseudo-equatorial orientation. The other five forms in the B class present the NHCOPh group in a pseudoaxial disposition. The observation that the sizes

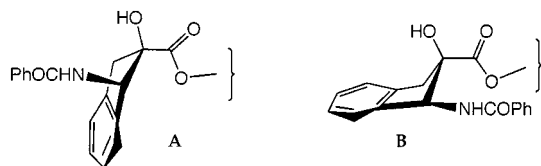


Figure 2. Envelope conformations of the indan system of **9a**, with the benzamido group pseudoaxial (A) or pseudoequatorial (B).

of the NOEs from 3' to both 2''a protons are unequal is consistent with an unequal distribution of conformations in which the benzamide group is partitioned between pseudoaxial and pseudoequatorial locations. Third, the available NOE data do not allow the NAMFIS deconvolution to distinguish (C2')C3'–NH(CO) rotamers in which this angle falls near -90 or $+90^\circ$ as is in the case for **9a3** and **9a4**.

Although the spectrum of **9b** was recorded in CDCl_3 , some insights on the two features highlighted for **9a** in Figure 1a can be gleaned for this compound as well. A Monte Carlo torsional MM3*/GBSA/ CHCl_3 search for **9b** delivered 328 conformations, which, when combined with seven NOEs and processed by a NAMFIS treatment, provided four conformations with estimated populations of 59, 35, 5, and 1%. The most populated form (**9b1**) is shown in Figure 1. Not surprisingly, it is very similar to the nonpolar conformation of Taxol, illustrating hydrophobic collapse between the C2 and C3' phenyl groups at the bottom of the figure. Unlike **9a**, however, the 4-OAc methyl group of **9b** is not found positioned above the tetralin aromatic ring. The C13–O and C1'–C2' bond torsions position the C3'–amide bond near the acetate instead. In accord, the chemical shift of this moiety is found at 2.22 ppm, almost identical to that in Taxol. At the same time, H3' evidences a strong NOE to the 4-acetate methyl indicating that H3' is directed into the concave hydrophobic region of the molecule. In consequence, the 6-ring protons at 2''a and 2''b are oriented *syn* to the C18 methyl of the terpenoid core as is the case for **9a**. Furthermore, in **9b** with a six-membered ring, the benzamide and C1' groups appear to be in pseudoequatorial and equatorial positions, respectively. The NOEs and *J*-couplings between the 2''a and 2''b protons are all consistent with this ring conformation. Thus, the preferred conformation of **9b** (Figure 1b) appears to be similar to **9a** with respect to the overall orientation of ring-fused C3' phenyl and the terpenoid core fragment.

Finally, do these conformations of **9a,b** correspond to potential 3-D templates for binding at the β -tubulin/Taxol binding site? Three competing proposals have emerged concerning the bioactive conformation of Taxol at the β -tubulin binding pocket. On the basis of solution NMR data and molecular modeling of nonataxel, Ojima and co-workers proposed a pharmacophore that incorporates the hydrophobically collapsed polar conformation of Taxol.^{7c} The same conformation in a different binding mode has been presented by Li et al. via REDOR NMR studies which utilized the electron crystallographic coordinates (EC) of β -tubulin obtained using Zn-stabilized, non-native protein sheets.^{10g} On the other hand, a pharmacophore model based on the hydrophobically collapsed nonpolar conformation of Taxol accommodates a wide range of taxoid and

epothilone SAR.^{7b} More recently, a computationally refined β -tubulin–paclitaxel complex, likewise taking advantage of the EC structure, has identified an extended conformation of the drug with a C13 side chain orientation related to the nonpolar conformation, the T-conformation, as most consistent with the electron crystallographic density of the $\alpha\beta$ -tubulin dimer.^{2c,10i,32} To correlate the **9a** conformers with these models, the A–C rings of each of the conformers **9a5**, **9a4**, and **9a1** (and **9a3**) (Table 2) have been superimposed on the corresponding atoms in the structures of polar,²⁴ nonpolar,^{10b} and T-forms of Taxol, respectively.¹⁰ⁱ The spatial locations of the three phenyl rings at the C2 and C3' termini for each of the structure pairs are very similar. To the extent that these three motifs are candidates for Taxol binding in microtubules, **9a** and presumably **24a** are molecules that appear to sustain NMR compatible equilibrium mixtures in solution containing all of them. Thus, although C2'–C3' torsional opportunities have been severely limited in **9a** and **24a**, the overall structures have compensated by adjustments around C1'–C2' and C3'–N. Indeed, while the local geometries of **9a** conformers differ from those of Taxol, the whole-molecule properties as seen externally (e.g. by a receptor cavity surface) have not been significantly affected. Consequently, although cyclization around C2' and C3' induces an unusual geometry at the terminus of the C13 side chains in **9a** and **24a**, the capacity of the compounds to adopt each of the three proposed Taxol binding conformers implies that the present series of constrained Taxol analogues cannot distinguish among the protein binding possibilities within the context of ligand considerations alone. In fact, this observation appears to be more broadly based. The NAMFIS study of Taxol in CDCl_3 likewise extracted members of the three conformational families.^{10h}

Summary and Conclusions

The introduction of a tether between C2' and the *ortho*-position of the C3' phenyl ring in Taxol and Taxotere produces compounds that are only slightly less active than Taxol in both tubulin polymerization and cytotoxicity assays (Table 1). Tolerance for structural deviation, however, is not high. Both tether lengthening and stereoinversion at C2' and C3' compromise activity. Conformational analysis coupled to 2-D NMR through the NAMFIS procedure illustrates that the active structures, **9a** and presumably **24a**, are characterized by a family of rapidly interconverting conformations. Among the seven conformers of **9a** compatible with solution NMR properties are found all three major types: polar, nonpolar, and extended conformations. The extended category constitutes 73% of the total mixture, while 59% of this fraction (47% of the total) is found in the T-form (i.e. **9a1**, **9a3**, and **9a7**).

Above we reviewed recent reports concerning the three hypotheses for the binding conformation of Taxol at the β -tubulin binding site. Two of them, the polar and nonpolar conformers, derive from pharmacophore models that consider the SAR of the ligands alone as a guide to the shape of the protein binding site. The fact that both nonpolar^{7b} and polar^{7c} models are able to correlate a large body of taxoid and epothilone SAR illustrates that such constructs do not converge to a unique view of the protein–ligand complex. The situa-

tion is parallel to the point expressed above concerning **9a**. In the absence of a constraining protein framework, individual ligands can adopt a range of relatively low energy conformations. Thus, in the present context, we believe that while pharmacophore models are useful, they incorporate significant limitations in their abilities to predict the bioactive conformation. This leaves the Li et al. proposal as the primary support for the polar conformation based on REDOR measurements within the tubulin–ligand complex.^{10g} However, T-Taxol likewise fulfills the geometric requirements of these measurements.³² Since the polar conformation does not fit the electron crystallographic density at the binding cavity of β -tubulin while the T-conformer does,¹⁰ⁱ we currently favor the latter as the best candidate for the bioactive conformation of taxoid drugs. Under this assumption, the dominant conformation of the constrained analogue **9a** (**9a1**) is superbly suited to mimic T-taxol in the binding site. As mentioned above, docking experiments with this structure²⁸ and a refined model of $\alpha\beta$ -tubulin are in full accord with this viewpoint.

Biological analogues of Taxol belonging to six distinct structural types have been discovered within the natural product pool (epothilones,^{6a} discodermolide,^{6b} eleuthisides,^{6c} rhazinilam,^{6d} laulimalides,^{6e} WS9885B,^{6f} and polyisoprenylated benzoylphloroglucinols^{6g}). A structurally simple mimic of Taxol has also been discovered while screening a library of synthetic compounds for antimetabolic activity,³³ and a competitive inhibitor of Taxol binding to microtubules has been reported.³⁴ All these compounds share a common recognition site on tubulin, and an enormous amount of work has been devoted to the identification of a common pharmacophore, assessing the structural elements responsible for this type of activity. The discovery of conformationally constrained analogues of Taxol substantially retaining the biological activity of the natural product is a significant addition to this research database and underscores the relevance of conformational point mutations to focus on the 3-D elements underlying the microtubule-stabilizing activity of taxoids.

Experimental Section

General Methods. Anhydrous conditions were achieved (when indicated) by flame-drying flasks and equipments. Reactions were monitored by TLC on Merck 60 F254 (0.25 mm) plates, which were visualized with 5% H₂SO₄ in EtOH and heating. Merck silica gel (70–230 mesh) was used for open-column chromatography (CC). A Waters microPorasil HP hypersyl column, 5 μ m, 200 \times 2.1 mm was used for HPLC, with detection by a Waters diode matrix DAD detector. Melting points were obtained on a Büchi SMP-20 apparatus and are uncorrected. ¹H NMR (300 MHz) and ¹³C NMR (75 MHz) spectra were recorded on a Bruker AC-300 spectrometer at 25 °C. ROESY spectra were recorded at 25 °C in DMSO-*d*₆ and NOESY spectra were recorded at –10 °C in DMSO-*d*₆–D₂O (3:1) on a Bruker AM-500 NMR spectrometer (500.13 MHz for ¹H). The spectra were fully assigned using HMBC on a Bruker Advance 400 (400.13 MHz for ¹H). The purity of all the final products (**9a**, **9b**, **20**, **24a** and **24b**) was assayed by HPLC on a Water microPorasil column (0.8 \times 30 cm), with detection by a Waters differential refractometer 340, using hexanes–EtOAc 4:6 (system A) and CHCl₃–acetone 3:1 (system B) as eluant. The values of *t*_R and purity were as follows: **9a**: *t*_R(A) = 14.8 min, *t*_R(B) = 19.3 min, purity 97%; **9b**: *t*_R(A) = 15.0 min, *t*_R(B) = 19.6 min, purity 98%; **20**: *t*_R(A) = 14.7 min, *t*_R(B) = 19.0 min, purity 96%; **24a**: *t*_R(A) = 14.3 min, *t*_R(B) = 19.2 min, purity 97%; **24b**: *t*_R(A) = 14.5 min, *t*_R(B) = 19.5 min, purity 96%.

(B) = 19.2 min, purity 97%; **24b**: *t*_R(A) = 14.5 min, *t*_R(B) = 19.5 min, purity 96%.

Biological Assays. Cytotoxicity and tubulin binding were carried out according to established literature protocols.³⁵

Materials. Commercially available reagents and solvents were used without further purification. CH₂Cl₂ was dried by distillation from CaH₂ and THF by distillation from N-benzophenone. 10-Deacetylbaconin III was a generous gift from Indena, Milano, Italy. The tethered cinnamates **3a**, **b** were prepared according to literature procedures.^{36,37}

Synthesis of Ethyl 2,2'-Methylidene-N-benzoylphenylisoserine (5a) and Ethyl 2,2'-Ethylidene-N-benzoylphenylisoserine (5b) via Asymmetric Aminohydroxylation. Synthesis of 5b as Representative. (a) To a stirred solution of benzyl carbamate (2.32 g, 15.3 mmol) in 2-propanol (20 mL), a solution of NaOH (604 mg) in water (37 mL), *tert*-butyl hypochlorite (1.73 mL) and (DHQ)₂PHAL (198 mg) in 2-propanol (17.3 mL) were sequentially added. After stirring at room temperature for 10 min, ethyl 3,4-dihydronaphthalene-2-carboxylate (1 g, 4.95 mmol) was added, followed by K₂O₂(OH)₄ (73 mg). After stirring at room temperature for 7 h, the reaction was worked up by cooling in an ice bath and addition of saturated Na₂SO₃ (49.5 mL). After further stirring for 15 min, the reaction mixture was extracted with EtOAc, and the organic phase was washed with brine, dried (Na₂SO₄) and evaporated. The residue was chromatographed on silica gel (hexanes–EtOAc 4:1) to give 610 mg **4b** as a gum (33%): [α]_D²⁵ ca. 0 (CHCl₃, *c* 1.0); IR (neat) 1740, 1650, 1250, 1010, 990 cm^{–1}; HRMS *m/z* 369.1566 (calcd for C₂₁H₂₃NO₅, 369.1576); ¹H NMR (300 MHz, CDCl₃) δ 8.03 (br m, 1H), 7.52 (br m, 1H), 7.30 (m, 2H), 5.13 (s, 1H), 4.38 (br d, *J* = 5.9 Hz, 1H), 4.28 (br s, 1H), 4.20 (q, *J* = 7.4 Hz, 2H), 3.11 (m, 1H), 2.70 (m, 1H), 2.23 (m, 1H), 1.20 (t, *J* = 7.4 Hz, 3H).

(b) To a solution of **4b** (547 mg, 1.49 mmol) in AcOH (23 mL), ammonium formate (375 mg) and 10% Pd on charcoal (257 mg) were added. After standing at room temperature for 4.5 h, the reaction mixture was filtered over Celite and evaporated under reduced pressure. The residue was partitioned between aqueous saturated NaHCO₃ and EtOAc, and the organic phase was dried (Na₂SO₄) and evaporated. The residue was dissolved in CH₂Cl₂ (5 mL), and sequentially treated with an aqueous solution of NaHCO₃ (191 mg in 5 mL) and benzoyl chloride (166 μ L, 1.43 mmol, 1.2 mol equiv). After stirring at room temperature for 3 h, the reaction was worked up by extraction with CH₂Cl₂. The organic phase was dried (Na₂SO₄) and evaporated. The residue was purified by CC (hexanes–EtOAc gradient, from 8:2 to 7:3) to give 354 mg **5b** (70% from **4b**), having [α]_D²⁵ ca. 0. For the other physical and spectroscopic data of **5b**, see **14**. The optical purity of **5a**, **b** was established as detailed for **10a** (see infra), and the observed ee were ca. 0 and <10%, respectively. Coupling of **5a**, **b** to 7-triethylsilylbaconin was carried out as described for **14** (see infra), employing a 2-fold excess of acid compared to **8**.

(1S,2R)-Ethyl 1,2-Dihydroxyindan-2-carboxylate (10a). To a solution of ADMix- α (14 g) in water–*tert*-butyl alcohol (1:1, 100 mL), ethyl indene-2-carboxylate (1.88 g, 10 mmol) was added in small portions over 5 min. After stirring at room temperature overnight, the reaction was worked up by the addition of solid Na₂SO₃ (12 g), stirring at room temperature for 1 h, and extraction with CH₂Cl₂. After drying (MgSO₄), filtration, and removal of the solvent, the residue was purified by CC (hexanes–EtOAc 8:2) to afford 1.4 g (64.5%) **10a** as a viscous yellowish oil: [α]_D²⁵ –15.0 (CHCl₃, *c* 1.0); IR (neat) 3400, 1738, 1370, 1250, 1220 cm^{–1}; HRMS *m/z* 222.0886 (calcd for C₁₂H₁₄O₄, 222.0892); ¹H NMR (300 MHz, CDCl₃) δ 7.50–7.18 (m, H-4, H-5, H-6, H-7), 5.37 (br s, H-1), 4.34 (q, *J* = 7.2 Hz, OEt), 3.78 (s, 2-OH), 3.50 (d, *J* = 16.2 Hz, H-3a), 3.10 (d, *J* = 16.2 Hz, H-3b), 2.89 (br s, 1-OH), 1.34 (t, *J* = 7.2 Hz, OEt). The optical purity of **10a** was determined as follows: to a cooled (0 °C) solution of **10a** (10 mg, 0.045 mmol) in dry THF (0.5 mL) TEA (9.4 μ L, 6.83 mg, 0.067 mmol, 1.25 mol equiv) and methylchloroformate (10.7 μ L, 10.9 mg, 0.05 mmol, 1.1 mol equiv in 0.5 mL dry THF) were added dropwise. After stirring 1 h at 0 °C, the cooling bath was removed, and stirring

was continued for 1 h, during which a white precipitate was formed. The reaction was then worked up by removal of the solvent and partition between Et₂O and 10% NaOH. After drying (MgSO₄) and evaporation, the residue was analyzed by HPLC (hexanes–EtOAc 95:5 as eluant; flow 0.7 mL/min), obtaining two peaks having identical UV spectra at *t_r* = 3.01 and 4.33, in a 96:4 ratio (ee = 92%): ¹H NMR (major isomer, 300 MHz, CDCl₃) δ 7.31 (m, 4H), 6.14 (s, 1H), 4.58 (dt, *J* = 10.7, 4.6 Hz, 1H), 4.33 (q, *J* = 7.1 Hz, 2H), 3.53 (d, *J* = 16.2 Hz, 1H), 3.19 (d, *J* = 16.2 Hz, 1H), 2.10 (m, 1H), 1.98 (m, 1H), 1.70 (m, 2H), 1.44 (m, 2H), 1.32 (t, *J* = 7.1 Hz, 3H), 1.12 (m, 2H), 0.95 (d, *J* = 7.0 Hz, 3H), 0.89 (d, *J* = 5.8 Hz, 3H), 0.81 (d, *J* = 5.8 Hz, 3H).

(1R,2S)-Ethyl 1-Bromo-2-benzoyloxyindan-2-carboxylate (11). To a solution of **10a** (3.02 g, 13.6 mmol) in dry CH₂Cl₂ (25 mL), *p*-toluenesulfonic acid monohydrate (25 mg, 0.136 mmol) and trimethyl orthobenzoate (3.04 mL, 3.22 g, 17.7 mmol, 1.3 mol equiv) were added. After stirring at room temperature for 3 h, the solvent was removed, leaving a yellowish oil. The latter was dissolved in dry CH₂Cl₂ (25 mL) and cooled to –15 °C. Acetyl bromide was then added (1.71 mL, 2 g, 16.3 mmol, 1.1 mol equiv). After stirring at –15 °C for 3 h, further trimethyl orthobenzoate (0.29 mL) and acetyl bromide (0.16 mL) were added, and stirring was continued at –15 °C for 1 h. The cooling bath was then removed, and the reaction mixture was allowed to warm to room temperature, and worked up by evaporation. The residue was purified by CC (hexanes–EtOAc gradient, from 95:5 to 9:1) to afford **11** as a foam (3.80 g, 72%): ¹H NMR (200 MHz, CDCl₃) δ 7.93 (Bz AA'), 7.60–7.20 (m, Bz BB' + H-4, H-5, H-6, H-7), 5.68 (s, H-1), 4.33 (q, *J* = 7.5 Hz, OEt), 4.27 (d, *J* = 17.6 Hz, H-3a), 3.46 (d, *J* = 17.6 Hz, H-3b), 1.30 (t, *J* = 7.5 Hz, OEt).

(1S,2R)-Ethyl 1-Benzoylamino-2-hydroxyindan-2-carboxylate (12). To a solution of **11** (4 g, 10.3 mmol) in dry DMF (16 mL), an excess NaN₃ (2.68 g, 41 mmol) was added, and the solution was heated at 50 °C for 36 h. The reaction was worked up by dilution with Et₂O (50 mL) and washing with water (3 × 40 mL). After drying (MgSO₄) and filtration, the organic phase was evaporated, and the residue dissolved in dry EtOH (40 mL) and hydrogenated at ambient pressure in the presence of 10% Pd on charcoal (1.2 g) for 36 h. After filtration, the solution was left standing at room temperature for 48 h, and then evaporated. The residue was purified by CC (silica gel, hexanes–EtOAc gradient, from 85:15 to 7:3) to get **12** (700 mg, 21%) as a foam: [α]_D²⁵ +11 (CHCl₃, *c* 1.1); IR (KBr) 3391, 1731, 1651, 1580, 1519, 1339, 1231 cm⁻¹; LC-MS (ESI) 348.0 (M + Na⁺); ¹H NMR (300 MHz, CDCl₃) δ 7.80 (Bz AA'), 7.40–7.60 (m, Bz BB', Bz C), 7.26 (br s, H-4, H-5, H-6, H-7), 6.80 (d, *J* = 9.3 Hz, NH), 6.09 (d, *J* = 9.3 Hz, H-1), 4.36 (q, *J* = 7.2, OEt), 3.64 (d, *J* = 16.3 Hz, H-3a), 3.14 (d, *J* = 16.3 Hz, H-3b), 1.35 (t, *J* = 7.2 Hz, OEt); ¹³C NMR (75.4 MHz, CDCl₃) δ 175.0 (s), 167.7 (s), 140.0 (s), 139.0 (s), 133.9 (s), 131.8 (d), 128.6 (d), 128.4 (d), 127.4 (d), 127.2 (d), 124.9 (d), 123.9 (d), 82.3 (s), 63.0 (d), 61.1 (t), 43.8 (t), 14.1 (q).

2',2''-Methylenepaclitaxel (9a). To a solution of **12** (100 mg, 0.31 mmol, 2 mol equiv) in dry toluene (2.5 mL), pyridinium *p*-toluenesulfonate (PPTS; 5 mg) and a solution of 2,4-dimethoxybenzaldehyde dimethylacetal (140 mg, excess) in dry toluene (0.5 mL) were added. The reaction was refluxed in a Dean–Stark apparatus for 2 h, and then worked up by removal of the solvent and partition between CH₂Cl₂ and water. The organic phase was dried (MgSO₄), filtered and evaporated. The residue was dissolved in methanol (4.5 mL) and a solution of K₂CO₃ (103 mg) in water (2.2 mL) was added. After stirring at room temperature for 30 min., the reaction was worked up by removal of the solvent and partition between water and EtOAc. The aqueous phase was acidified with 5% KHSO₄ and extracted with EtOAc. After washing with brine, drying (MgSO₄) and evaporation, the unstable residue was dissolved in dry toluene (5 mL) and directly coupled with 7-triethylsilylbaccatin III³⁸ (108.6 mg, 0.155 mmol, 0.5 mol equiv) in the presence of DMAP (16.5 mg, 0.135 mmol) and DCC (76 mg, 0.37 mmol). After stirring at room temperature for 6 h, the reaction was worked up by evaporation, and the residue was

taken up in 0.1 M methanolic HCl. After stirring 1 h at room temperature, the reaction was evaporated, and the residue purified by CC (silica gel, 2% MeOH in hexanes–EtOAc 1:1) to afford 47 mg (35% from **12**) **9a** as a colorless powder: mp 254 °C; [α]_D²⁵ –48 (CHCl₃, *c* 0.70); IR (KBr) 1745, 1457, 1383, 1203, 720 cm⁻¹; HRMS-FAB *m/z* 866.3386 (calcd for C₄₈H₅₁NO₁₄ + H⁺ 866.3388); ¹H NMR (300 MHz, CDCl₃) δ 8.08 (AA' OBz), 7.80 (AA' NHBz), 7.60–7.40 (m, BB' OBz, C OBz, BB' NHBz, C NHBz), 7.33 (m, H-3'', H-4'', H-5'', H-6''), 6.78 (d, *J* = 9.0 Hz, NH), 6.42 (br t, *J* = 9.2 Hz, H-13), 6.29 (s, H-10), 6.10 (d, *J* = 9.0 Hz, H-3'), 5.69 (d, *J* = 7.3 Hz, H-2), 4.85 (br d, *J* = 9.9 Hz, H-5), 4.37 (dd, *J* = 10.8, 6.8 Hz, H-7), 4.25 (d, *J* = 8.4 Hz, H-20α), 4.16 (d, *J* = 8.4 Hz, H-20β), 3.83 (d, *J* = 16.5 Hz, 2',2''-CH₂α), 3.79 (d, *J* = 7.3 Hz, H-3), 3.30 (d, *J* = 16.5 Hz, 2',2'' CH₂β), 2.50 (ddd, *J* = 14.9, 9.9, 6.8 Hz, H-6α), 2.44 (dd, *J* = 15.4, 9.2 Hz, H-14b), 2.35 (dd, *J* = 15.4, 9.2 Hz, H-14a), 2.24 (s, 10-OAc), 1.93 (br s, H-18), 1.87 (s, 4-OAc), 1.85 (ddd, *J* = 14.9, 11.0, 2.2 Hz, H-6b), 1.67 (s, H-19), 1.30 (s, H-17), 1.16 (s, H-16); ¹³C NMR (75 MHz, CDCl₃) δ 203.6 (s, C-9), 175.1 (s, C-1'), 171.3 (s, 10-OAc), 170.4 (s, 4-OAc), 168.0 (s, NHBz), 166.9 (s, OBz), 142.0 (s, C-12), 139.1 (s, C-2''), 138.8 (s, *i*-NHBz), 133.6 (d, *p*-OBz), 133.4 (s, C-1''), 133.1 (s, C-11), 132.1 (d, C-4''), 130.2 (d, *o*-OBz), 129.1 (d, C-5''), 129.1 (s, *i*-OBz), 128.7 (d, *m*-NHBz), 128.7 (d, *m*-OBz), 127.9 (d, *p*-NHBz), 127.2 (d, *o*-NHBz), 125.2 (d, C-3''), 123.8 (d, C-6''), 84.4 (d, C-5), 82.1 (d, C-2'), 81.2 (s, C-4), 78.9 (s, C-1), 76.6 (t, C-20), 75.6 (d, C-10), 74.9 (d, C-2), 72.6 (d, C-13), 72.3 (d, C-7), 61.7 (d, C-3'), 58.7 (s, C-8), 45.6 (d, C-3), 43.9 (t, 2'(2'')-CH₂), 43.3 (s, C-15), 35.7 (t, C-6 + C-14), 26.9 (q, C-17), 21.9 (q, C-16), 21.7 (4-OAc), 20.9 (10-OAc), 15.0 (q, C-18), 9.5 (q, C-19).

(1S,2R)-Ethyl 1,2-Dihydroxytetrahydronaphthalene-2-carboxylate (10b). To a solution of Admix-α (14 g) in water–*tert*-butyl alcohol (1:1, 100 mL), ethyl 3,4-dihydronaphthalene-2-carboxylate (2.02 g, 10 mmol) was added in small portions over 5 min. After stirring at room temperature overnight, the reaction was worked up by addition of solid Na₂SO₃ (12 g), stirring at room temperature for 1 h, and extraction with CH₂Cl₂. After drying (MgSO₄), filtration, and removal of the solvent, the residue was purified by CC (hexanes–EtOAc 8:2) to afford 1.8 g (77%) **10b** as an amorphous solid: [α]_D²⁵ –42.9 (CHCl₃, *c* 1.0); IR (Nujol) 3413, 1720, 1376, 1269, 1235 cm⁻¹; EI-MS (70 eV) 236 (M⁺), 218, 200, 172, 162, 120; ¹H NMR (300 MHz, CDCl₃) δ 7.58 (d, *J* = 7.5, H-9), 7.20 (m, H-7, H-8), 7.09 (d, *J* = 7.3 Hz, H-5), 5.00 (br d, *J* = 11.1 Hz, H-1), 4.31 (q, *J* = 7.1 Hz, OEt), 3.59 (s, 2-OH), 3.12 (ddd, *J* = 17.0, 12.5, 6.0 Hz, H-4a), 2.74 (ddd, *J* = 17.0, 6.0, 2.0 Hz, H-4b), 2.56 (br d, *J* = 11.2 Hz, 1-OH), 2.20 (ddd, *J* = 13.7, 12.6, 6.0 Hz, H-3a), 2.02 (ddd, *J* = 13.7, 6.0, 2.0 Hz, H-3b), 1.32 (t, *J* = 7.1 Hz, OEt). The optical purity of **10b** was determined as described for **10a**, giving an ee value of 93%.

(1R,2S)-Ethyl 1-Bromo-2-hydroxytetrahydronaphthalene-2-carboxylate (13). To a stirred and cooled (0 °C) solution of **10b** (945 mg, 4.0 mmol) in dry CH₂Cl₂ (60 mL), pyridine (967 μL, 948 mg, 12 mmol, 3 mol equiv) and thionyl chloride (408 μL, 5.6 mmol, 1.4 mol equiv) were added. After stirring at 0 °C for 10 min., the reaction mixture was filtered on a silica gel pad, and evaporated. The crude sulfite was dissolved in acetonitrile (40 mL) and treated with NaIO₄ (1.284 g, 6 mmol, 1.5 mol equiv) and a solution of RuCl₃·H₂O (10 mg, 0.04 mmol) in water (8 mL). After stirring for 15 min at room temperature, the reaction was worked up by dilution with water, extraction with ether and filtration over silica gel. After drying (Na₂SO₄) and evaporation of the solvent, the crude and unstable sulfate was dissolved in acetone–water (15 mL, 1:1) and treated with an excess *n*Bu₄NBr (3.380 g, 10.4 mmol, 2.6 mol equiv). After stirring 2 h at room temperature the reaction was worked up by concentration under vacuum to remove most acetone and treatment with 20% H₂SO₄ (8.5 mL) and ether (10.5 mL). After vigorous stirring for 30 min., the phases were separated, and the aqueous layer was further extracted with ether. The pooled organic phases were dried (Na₂SO₄) and evaporated, and the residue was purified by CC (silica gel, hexanes–EtOAc 9:1) to give 243 mg **13** (20%) as an amorphous glass: EI-MS (70 eV) 301, 299 (M⁺), 274, 272, 220, 219; 169;

¹H NMR (300 MHz, CDCl₃) δ 7.35 (m, H-8), 7.19 (m, H-6, H-7), 7.12 (m, H-5), 5.19 (s, H-1), 4.31 (q, *J* = 7.1 Hz, OEt), 3.03 (m, H-4a, H-4b), 2.65 (m, H-3a), 2.16 (m, H-3b), 1.33 (t, *J* = 7.1 Hz, OEt).

(1*S*,2*R*)-Ethyl 1-Benzoylamino-2-hydroxytetrahydronaphthalene-2-carboxylate (14). To a stirred solution of **13** (543 mg, 1.82 mmol) in dry DMF, NaN₃ (471 mg, 7.24 mmol, 4 mol equiv) was added, and the solution was stirred 10 min. at 50 °C. The reaction was worked up by addition of ice and extraction with Et₂O. After drying (MgSO₄), the organic phase was evaporated, and the residue was purified by CC (silica gel, hexanes–EtOAc 4:1) to afford 60 mg (13%) of the corresponding azide. To a solution of the latter (284 mg, 1.19 mmol) in EtOAc (20 mL), Pd on charcoal (50 mg) was added, and the mixture was hydrogenated at room temperature and atmospheric pressure for 4 h. After filtration over Celite and evaporation, the residue was dissolved in CH₂Cl₂ (5 mL), and an aqueous solution of NaHCO₃ (191 mg in 5 mL) and benzoyl chloride (166 μL, 201 mg, 1.43 mmol, 1.2 mol equiv) were added. After vigorous stirring for 3 h, the phases were separated, and the aqueous phase was extracted with CH₂-Cl₂. The pooled organic phases were dried (Na₂SO₄) and evaporated, to afford 536 mg (87%) **14** as an amorphous solid: [α]_D²⁵ 45.2 (CHCl₃, *c* 1.4); IR (Nujol) 3385, 1730, 1655, 1340, 1225 cm⁻¹; LC–MS (ESI) 362.0; ¹H NMR (300 MHz, CDCl₃) δ 7.77 (m, 2H), 7.26 (m, 1H), 7.15 (m, 3H), 6.73 (d, *J* = 9.5 Hz, 1H), 5.86 (d, *J* = 9.5 Hz, 1H), 4.27 (m, 2H), 3.19 (ddd, *J* = 16.8, 12.8, 5.7 Hz, 1H), 2.83 (ddd, *J* = 16.8, 5.8, 2.0 Hz, 1H), 2.36 (ddd, *J* = 13.7, 12.8, 5.8 Hz, 1H), 2.04 (ddd, *J* = 13.7, 5.7, 2.2 Hz, 1H), 1.28 (t, *J* = 7.2 Hz, 3H).

2',2''-Ethylidenepaclitaxel (9b). To a solution of **14** (406 mg, 1.2 mmol, 2 mol equiv) in dry toluene (5 mL), PPTS (10 mg) and a solution of 2,4-dimethoxybenzaldehyde dimethylacetal (537 mg) in dry toluene (1 mL) were added. The reaction was refluxed in a Dean–Stark apparatus for 2 h, and then worked up by removal of the solvent and partition between CH₂Cl₂ and water. The organic phase was dried (MgSO₄), filtered and evaporated. The residue was dissolved in methanol (10 mL) and a solution of K₂CO₃ (395 mg) in water (8.5 mL) was added. After stirring at room temperature for 30 min., the reaction was worked up by removal of the solvent and partition between water and EtOAc. The aqueous phase was acidified with 5% KHSO₄ and extracted with EtOAc. After washing with brine, drying (MgSO₄) and evaporation, the unstable residue was dissolved in dry toluene (19 mL) and directly coupled with 7-triethylsilylbaccatin III (414 mg, 0.60 mmol) in the presence of DMAP (63 mg, 0.51 mmol) and DCC (291 mg, 1.42 mmol, 1.2 mol equiv). After stirring at room temperature overnight, the reaction was worked up by evaporation, and the residue was taken up in 0.1 M methanolic HCl. After stirring 1 h at room temperature, the reaction was evaporated, and the residue purified by CC (silica gel, 2% MeOH in hexanes–EtOAc 1:1) to afford 301 mg (29%) **9b** as a colorless powder: mp 254 °C; [α]_D²⁵ 3.3 (CHCl₃, *c* 0.73); IR (KBr) 1745, 1457, 1383, 1203, 720 cm⁻¹; HRMS–FAB *m/z* 880.3577 (calcd for C₄₉H₅₄NO₁₄ + H⁺ 880.3544); ¹H NMR (300 MHz, CDCl₃) δ 8.22 (AA' OBz), 7.71 (AA' NHBz), 7.60–7.40 (m, BB' OBz, C OBz, BB' NHBz), 7.34 (C NHBz), 7.23 (m, H-3'', H-4'', H-5'', H-6''), 6.76 (d, *J* = 9.6 Hz, NH), 6.35 (br t, *J* = 9.2 Hz, H-13), 6.26 (s, H-10), 5.96 (d, *J* = 9.0 Hz, H-3'), 5.66 (d, *J* = 7.3 Hz, H-2), 4.86 (br d, *J* = 8.9 Hz, H-5), 4.38 (dd, *J* = 10.8, 6.8 Hz, H-7), 4.25 (d, *J* = 8.4 Hz, H-20α), 4.20 (d, *J* = 8.4 Hz, H-20β), 3.80 (d, *J* = 7.3 Hz, H-3), 3.27 (m, 2',2''-ethylidene), 2.92 (dd, *J* = 16.8, 4.5 Hz, 2',2''-ethylidene), 2.48 (m, H-6α, H-14α, 2',2''-ethylidene), 2.32 (s, 10-OAc), 2.22 (s, 4-OAc), 2.20 (m, H-14β, 2',2''-ethylidene), 1.87 (br s, H-18), 1.85 (m, H-6β), 1.68 (s, H-19), 1.24 (s, H-17), 1.12 (s, H-16); ¹³C NMR (75 MHz, CDCl₃) δ 203.7 (s, C-9), 175.6 (s, C-1'), 171.3 (s, 10-OAc), 171.0 (s, 4-OAc), 167.3, 167.1 (s, NHBz + OBz), 142.1 (s, C-12), 135.6 (s, C-2''), 133.8 (d, *p*-OBz), 133.7, 133.6 (s, NHBz + C-1'), 132.9 (C-11), 131.9 (d, *p*NBz), 130.4 (d, *o*-OBz), 129.2 (s, *i*-OBz), 128.8, 128.7 (d, *m*-NHBz + *m*-OBz), 127.6, 127.3, 127.1, 126.9 (d, C-3'' + C-4'' + C-5'' + C-6''), 84.5 (d, C-5), 81.1 (d, C-4), 79.2 (s, C-1), 76.7 (t, C-20), 75.5 (d, C-10), 75.1 (d, C-2 + C-2'),

72.3, 72.2 (d, C-13 + C-7), 58.6 (s, C-8), 51.9 (d, C-3'), 45.5 (d, C-3), 43.2 (s, C-15), 35.8, 35.6 (t, C-6, C-14), 31.8 (t, 2',2''-ethylidene), 26.9 (q, C-17), 24.6 (t, 2',2''-ethylidene), 22.7 (OAc), 22.3 (C-16), 20.9 (OAc), 14.9 (C-18), 9.6 (C-19).

2',2''-Methylene-2',3'-epipaclitaxel (20). To a solution of **19** (138 mg, 0.31 mmol, 2 mol equiv, prepared from **3a** as described for **9a** but employing ADMix-β for the dihydroxylation step (ee of the diol: 92%)) in dry toluene (12.5 mL), DMAP (37 mg, 0.31 mmol, 2 mol equiv), 7-triethylsilylbaccatin III (**8**) (108 mg, 0.155 mmol) and DCC (166 mg, 0.8 mmol, 5.1 mol equiv) were added, and the reaction was stirred at room temperature overnight and then heated at 70 °C for 1 h. After cooling, the reaction was filtered, and evaporated. The residue was taken up in 0.1 M methanolic HCl (21 mL). After stirring 1.5 h at room temperature, the reaction was evaporated, and the residue purified by CC (silica gel, hexanes–EtOAc 1:1) to afford 31 mg (11%) **20** as a foam: [α]_D²⁵ –100 (CHCl₃, *c* 0.80); IR (KBr) 1716, 1653, 1488, 1373, 1241, 751 cm⁻¹; HRMS–FAB *m/z* 866.3380 (calcd for C₄₈H₅₁NO₁₄ + H⁺ 866.3388); ¹H NMR (300 MHz, CDCl₃) δ 8.08 (AA' OBz), 7.63–7.40 (overlapped m, AA' NHBz, BB' OBz, C OBz, BB' NHBz, C NHBz), 7.33 (m, H-3'', H-4'', H-5'', H-6''), 6.81 (d, *J* = 8.0 Hz, NH), 6.38 (br t, *J* = 8.8 Hz, H-13), 6.28 (s, H-10), 6.18 (d, *J* = 8.8 Hz, H-3'), 5.66 (d, *J* = 7.1 Hz, H-2), 4.88 (br d, *J* = 9.6 Hz, H-5), 4.40 (dd, *J* = 10.8, 6.7 Hz, H-7), 4.25 (d, *J* = 8.8 Hz, H-20α), 4.12 (d, *J* = 8.8 Hz, H-20β), 3.80 (d, *J* = 7.3 Hz, H-3), 3.65 (d, *J* = 16.3 Hz, 2',2''-CH₂α), 3.27 (d, *J* = 16.3 Hz, 2'' CH₂β), 2.51 (m, H-6α), 2.28 (m, H-14a + H-14b), 2.21 (s, 10-OAc), 2.00 (br s, H-18), 1.91 (s, 4-OAc), 1.83 (m, H-6β), 1.65 (s, H-19), 1.30 (s, H-17), 1.14 (s, H-16); ¹³C NMR (75 MHz, CDCl₃) δ 203.7 (s, C-9), 175.1 (s, C-1'), 171.2 (s, 10-OAc), 169.8 (s, 4-OAc), 167.5 (s, NHBz), 167.2 (s, OBz), 142.8 (s, C-12), 139.7 (s, C-2''), 138.2 (s, *i*-NHBz), 133.8 (d, *p*-OBz), 132.5 (s, C-1'), 132.0 (d, C-4''), 130.9 (s, C-11), 130.0 (d, *o*-OBz), 129.1 (d, C-5''), 129.0 (s, *i*-OBz), 128.7 (d, *m*-NHBz), 128.7 (d, *m*-OBz), 128.0 (d, *p*-NHBz), 127.1 (d, *o*-NHBz), 124.9 (d, C-3''), 124.4 (d, C-6''), 84.5 (d, C-5), 82.2 (d, C-2'), 81.2 (s, C-4), 79.4 (s, C-1), 76.5 (t, C-20), 75.5 (d, C-10), 75.0 (d, C-2), 72.9 (d, C-13), 72.2 (d, C-7), 61.1 (d, C-3'), 58.6 (s, C-8), 45.5 (d, C-3), 44.5 (t, 2'(2'')-CH₂), 43.2 (s, C-15), 35.9, 35.6 (t, C-6 + C-14), 27.0 (q, C-17), 22.1 (q, C-16), 21.7 (4-OAc), 20.8 (10-OAc), 15.1 (q, C-18), 9.6 (q, C-19).

Synthesis of (±)-2,2'-Methylidene-*N*-(*tert*-butoxycarbonyl)phenylisoserine (21a) and (±)-2,2'-Ethylidene-*N*-(*tert*-butoxycarbonyl)phenylisoserine (21b). Synthesis of 21b as Representative. Compound (±)**4b** was reductively deacylated as described for the synthesis of **5b**. To a solution of the crude deacylated product (307 mg, 1.3 mmol) in CH₂Cl₂ (4.5 mL), aqueous NaHCO₃ (158 mg in 4.5 mL) and *tert*-butoxycarbonylpyrocarbonate (Boc₂O; 284 mg, 1.3 mmol, 1 mol equiv) were added. After stirring at room temperature for 5 h, further solid NaHCO₃ (23 mg) and Boc₂O (38 mg) were added, and stirring was continued overnight. After separation of the two phases, the water phase was extracted with CH₂-Cl₂, and the pooled organic phases were dried (Na₂SO₄) and evaporated. The residue was purified by CC (hexanes–EtOAc gradient, from 9:1 to 8:2), 289 mg **21b** were obtained (66%) as an amorphous solid: [α]_D²⁵ 9.2 (CHCl₃, *c* 1.1); IR (Nujol) 1731, 1678, 1528, 1250, 1173 cm⁻¹; LC–MS (ESI) 358.4 (M + Na⁺); ¹H NMR (300 MHz, CDCl₃) δ 7.26 (m, 1H), 7.16 (m, 2H), 7.09 (m, 1H), 5.26 (br d, *J* = 10.2 Hz, 1H), 5.07 (br d, *J* = 10.2 Hz, 1H), 4.27 (m, 2H), 3.12 (ddd, *J* = 16.8, 12.7, 5.7 Hz, 1H), 2.76 (ddd, *J* = 16.8, 6.0, 2.2 Hz, 1H), 2.29 (ddd, *J* = 13.5, 12.7, 6.0 Hz, 1H), 1.97 (ddd, *J* = 13.5, 5.7, 2.2 Hz, 1H), 1.31 (t, *J* = 7.1 Hz, 3H). Physical data for **21a** (43% yield from **5a**): gum; IR (neat) 1735, 1680, 1610, 1510, 1247, 1089 cm⁻¹; HRMS *m/z* 321.1588 (calcd for C₁₇H₂₃NO₅, 321.1576); ¹H NMR (300 MHz, CDCl₃) δ 7.23 (m, 4H), 5.53 (br d, *J* = 9.8 Hz, 1H), 5.13 (br d, *J* = 9.8 Hz, 1H), 4.31 (q, 2H), 3.60 (br s, 1H), 3.56 (d, *J* = 16.1 Hz, 1H), 3.06 (d, *J* = 16.1 Hz, 1H), 1.45 (s, 9H), 1.32 (t, *J* = 6.9 Hz, 3H); ¹³C NMR (75.4 MHz, CDCl₃) δ 174.9 (s), 155.8 (s), 140.1 (s), 138.9 (s), 128.2 (d), 127.2 (d), 124.8 (d), 123.9 (d), 82.3 (s), 79.8 (s), 62.7 (d), 62.6 (t), 43.1 (t), 28.3 (q), 14.1 (q).

2',2''-Methylenedocetaxel (24a). (a) **Amido alcohol protection and ester hydrolysis of 21a:** To a solution of **21a** (321 mg, 1 mmol) in dry toluene (6.5 mL) PPTS (14 mg) and 2,4-dimethoxybenzaldehyde dimethylacetal (424 mg, excess) were added, and the solution was refluxed in a Dean–Stark apparatus for 2 h. After evaporation of the solvent, the residue was taken up in CH_2Cl_2 and washed with brine. The organic phase was dried (Na_2SO_4) and evaporated. The residue was filtered through a short column of silica gel to remove the excess acetal, and then hydrolyzed by treatment with K_2CO_3 in methanol (234 mg in 5 mL). After stirring 30 min at room temperature, the reaction was worked up by evaporation, and the residue taken up in a mixture of EtOAc and water (1:1, 10 mL). The water phase was next acidified with 5% KHSO_4 and extracted with EtOAc. After drying (Na_2SO_4) and removal of the solvent, crude **22a** was obtained (356 mg, 80% from **21a**) as an unstable glass, directly used for the coupling step.

(b) **Coupling and deprotection:** To a stirred solution of **22a** (450 mg, 1.02 mmol, 1.6 mol equiv) and 7,10-bis(trichloroacetyl)-10-deacetylbaecatin III (**23**)³⁹ (576 mg, 0.64 mmol) in dry toluene (22 mL), DMAP (67 mg, 0.55 mmol, 0.86 mmol) and DCC (305 mg, 1.48 mmol, 2.3 mol equiv) were added, and the mixture was stirred at room temperature overnight. The reaction was worked up by evaporation, and the residue was treated with 0.1 N methanolic HCl (5 mL) to hydrolyze the acetal moiety on the side chain. After evaporation, the residue was dissolved in dry methanol (22.5 mL) and treated with zinc (previously activated by treatment with dilute HCl, filtration, and washing with MeOH, 600 mg) and AcOH (13.5 mL). After stirring at 60 °C for 2 h, the reaction mixture was filtered, evaporated, and partitioned between water and EtOAc. The organic phase was dried (Na_2SO_4) and evaporated. The residue was purified by CC (hexanes–EtOAc gradient, from 35:65 to 3:7) to afford 159 mg **24a** (17%) as a foam: $[\alpha]_D^{25} -47$ (CHCl_3 , c 0.70); IR (KBr) 3435, 1707, 1244, 1166, 1094, 1053, 1025 cm^{-1} ; HRMS-FAB m/z 820.3551 (calcd for $\text{C}_{44}\text{H}_{53}\text{NO}_{14} + \text{H}^+$ 866.3544); ^1H NMR (300 MHz, CDCl_3) δ 8.05 (AA' OBz), 7.55 (C OBz), 7.45 (BB' OBz), 7.27 (m, H-3'', H-4'', H-5'', H-6''), 6.36 (br t, $J = 8.9$ Hz, H-13), 6.29 (s, H-10), 5.67 (d, $J = 7.0$ Hz, H-2), 5.56 (d, $J = 9.6$ Hz, H-3'), 5.20 (s, H-10), 5.16 (d, $J = 9.6$ Hz, NH), 4.84 (br d, $J = 9.0$ Hz, H-5), 4.24 (d, $J = 8.7$ Hz, H-20 α), 4.19 (m H-7), 4.14 (d, $J = 8.7$ Hz, H-20 β), 3.89 (d, $J = 7.0$ Hz, H-3), 3.73 (d, $J = 16.5$ Hz, 2',2''- $\text{CH}_2\beta$), 3.20 (d, $J = 16.5$ Hz, 2,2'' $\text{CH}_2\alpha$), 2.50 (m, H-6 α), 2.29 (m, H-14 α + H-14 β), 1.96 (br s, H-18), 1.89 (s, 4-OAc), 1.80 (m, H-6 β), 1.73 (s, H-19), 1.42 (s, NHBoc), 1.26 (s, H-17), 1.12 (s, H-16); ^{13}C NMR (75 MHz, CDCl_3) δ 211.4 (s, C-9), 175.1 (s, C-1'), 170.4 (s, 4-OAc), 167.0 (s, OBz), 156.2 (s, NHBoc), 139.5, 138.5, 138.4, 135.9 (s, C-11, C-12, C-1', C-2'), 133.7 (d, *p*-OBz), 130.1 (d, *o*-OBz), 129.1 (s, *i*-OBz), 128.7 (d, *m*-OBz), 128.8, 127.6, 125.0, 123.9 (d, C-3'' + C-4'' + C-5'' + C-6''), 84.2 (d, C-5), 82.2 (d, C-2), 81.1 (s, C-4), 80.29 (s, NHBoc), 78.8 (s, C-1), 76.7 (t, C-20), 74.8 (d, C-2), 74.6 (d, C-10), 72.4 (d, C-13), 72.1 (d, C-7), 63.1 (d, C-3'), 58.7 (s, C-8), 46.4 (d, C-3), 43.3 (s, C-15), 43.2 (t, 2'-(2'')- CH_2), 37.1 (t, C-6), 35.8 (t, C-14), 28.3 (q, Boc), 26.6 (q, C-17), 21.7 (q, OAc), 20.72 (q, C-16), 14.6 (q, C-18), 9.8 (q, C-19).

2',2''-Ethylidenedocetaxel (24b). **21b** (530 mg) was protected, hydrolyzed and coupled with 7,10-bistrichloroacetyl-10-deacetylbaecatin III (**23**) as described for **21a**. After deprotection, the final product was purified by CC (hexanes–EtOAc 1:1) to afford 9 mg **24b** (4% from **22b**) as a foam: $[\alpha]_D^{25} -26.9$ (CHCl_3 , c 0.5) (CHCl_3 , c 0.70); IR (KBr) 3450, 1740, 1715, 1660, 1640, 1240 cm^{-1} ; HRMS-FAB m/z 834.3695 (calcd for $\text{C}_{45}\text{H}_{55}\text{NO}_{14} + \text{H}^+$ 834.3701); ^1H NMR (300 MHz, CDCl_3) δ 8.13 (AA' OBz), 7.58 (C OBz), 7.48 (BB' OBz), 7.20 (m, H-3'', H-4'', H-5'', H-6''), 6.38 (br t, $J = 9.0$ Hz, H-13), 6.29 (s, H-10), 5.66 (d, $J = 7.2$ Hz, H-2), 5.34 (d, $J = 10.1$ Hz, H-3'), 5.18 (s, H-10), 5.12 (d, $J = 10.1$ Hz, NH), 4.86 (br d, $J = 9.3$ Hz, H-5), 4.25 (d, $J = 8.5$ Hz, H-20 α), 4.19 (m, H-7), 4.17 (d, $J = 8.5$ Hz, H-20 β), 3.91 (d, $J = 7.0$ Hz, H-3), 3.20 (m, 2',2''-ethylidene), 2.86 (dd, $J = 17.2$, 4.5 Hz, 2',2''-ethylidene), 2.53 (m, H-6 α), 2.38 (m, 2',2''-ethylidene), 2.27 (s, 4-OAc), 2.15 (m, H-14 α,β), 1.91 (br s, H-18), 1.82 (m, H-6 β), 1.74 (s, H-19), 1.32 (s, Boc), 1.26 (s, H-17), 1.11 (s, H-16); ^{13}C NMR (75 MHz, CDCl_3) δ 211.4 (s,

C-9), 175.7 (s, C-1'), 170.8 (s, 4-OAc), 167.1 (s, OBz), 156.1 (s, OBoc), 138.6, 135.7, 135.5, 134.5 (s, C-11, C-12, C-1', C-2'), 133.5 (d, *p*-OBz), 130.3 (d, *o*-OBz), 129.2 (s, *i*-OBz), 128.7 (d, *m*-OBz), 127.6, 127.3 (d, 3'-Ph), 127.0, 126.6 (d, C-3'' + C-4'' + C-5'' + C-6''), 84.3 (d, C-5), 81.0 (s, C-4), 79.8 (s, NHBoc), 79.0 (s, C-1), 76.8 (t, C-20), 75.2 (d, C-2), 74.9 (d, C-2), 74.4 (d, C-10), 72.1 (d, C-13, C,7), 57.6 (s, C-8), 53.4 (d, C-3'), 46.5 (d, C-3), 43.1 (s, C-15), 37.0 (t, C-6), 35.9 (t, C-14), 31.5 (t, 2',2''-ethylidene), 28.2 (q, NHBoc), 26.6 (q, C-17), 24.7 (t, 2',2''-ethylidene), 22.6 (q, OAc), 21.04 (q, C-16), 14.3 (q, C-18), 9.9 (q, C-19).

Computational Procedures. Structure **9a** was subjected to a Monte Carlo conformational search⁴⁰ with the MM3* force field and the GB/SA/H2O continuum model in MacroModel6.5 with default parameters.²⁹ The Monte Carlo treatment was employed since it is one of the most efficient procedures available for exploring the conformational energy surface of small to medium sized molecules.⁴¹ Similarly, the semianalytical GB/SA/H2O model was chosen to mimic polar solvent because it is well-parametrized for a range of organic structures.^{29b} At worst, the method dampens unrealistic gas-phase dipole–dipole interactions. Under these conditions, the **9a** search was run for a total of 5000 steps. The global minimum was located 6 times. The set of 1121 optimized conformers was treated to a NAMFIS conformer deconvolution analysis²⁸ by fitting 14 NOE-determined distances derived in DMSO- d_6 . The NOE cross-peak volumes were scaled by comparison with the volume of the H7–H10 cross-peak assigned a distance of 2.40 Å. The NAMFIS fitting procedure provided seven conformations with predicted populations ranging from 2–26%, i.e., 26, 21, 15, 15, 12, 10 and 2%, with a sum of square differences (SSD)²⁸ of 128. A Monte Carlo torsional search was likewise performed for the six-membered ring analogue **9b**, this time, however, with the MM3*/GBSA/CHCl₃ prescription.^{29c} The calculation delivered 328 conformations (global minimum found 49 times), which when combined with seven NOEs and processed by a NAMFIS treatment provided four conformations with estimated populations of 59, 35, 5 and 1% (SSD = 5). Consistent with the polarity of the solvent, the two most abundant conformers correspond to the “nonpolar” Taxol variant, while the less abundant structures are uncollapsed forms. All structures were visualized on SGI O2 workstations and further manipulated in MacroModel: for example, for evaluation of the ring-flip character of **9a** A and B as well as superposition of **9a** conformers with those of Taxol, Taxotere, and T-Taxol.

References

- (1) Three books have been devoted to the chemistry and medicinal chemistry of Taxol: (a) *Taxol: Science and Application*, Suffness, M., Ed.; CRC: Boca Raton, FL, 1995. (b) *Taxane Anticancer Agents: Basic Science and Current Status*, Georg, G. I., Chen, T. T., Ojima, I., Vyas, D. M., Eds.; American Chemical Society: Washington, DC, 1995. (c) *The Chemistry and Pharmacology of Taxol and its Derivatives*, Farina, V., Ed.; Elsevier: Amsterdam, 1995. For an earlier review, see: Nicolaou, K. L. C.; Dai, W. M.; Guy, R. K. *Chemistry and Biology of Taxol*. *Angew. Chem., Int. Ed. Engl.* **1994**, *33*, 15–44.
- (2) For major reviews, see: (a) Chen, S. H.; Farina, V. *Paclitaxel (Taxol) Chemistry and Structure–Activity Relationships*. In *The Chemistry and Pharmacology of Taxol and its Derivatives*, Farina, V., Ed.; Elsevier: Amsterdam, 1995; pp 165–253. (b) Georg, G. I. *The Medicinal Chemistry of Taxol*. In *Taxol: Science and Application*; Suffness, M., Ed.; CRC: Boca Raton, FL, 1995; pp 317–375. (c) Wang, M.; Cornett, B.; Nettles, J.; Liotta, D. C.; Snyder, J. P. *The Oxetane Ring of Taxol*. *J. Org. Chem.* **2000**, *65*, 1059–1068.
- (3) For a review, see: Guénard, D.; Guéritte-Voegelien, F.; Potier, P. *Taxol and Taxotere: Discovery, Chemistry, and Structure–Activity Relationships*. *Acc. Chem. Res.* **1993**, *26*, 160–167.
- (4) For a review, see: Ojima, I.; Lin, S.; Tao, W. *Recent Advances in the Medicinal Chemistry of Taxoids with Novel β -Amino Acid Side Chains*. *Curr. Med. Chem.* **1999**, *6*, 927–954.
- (5) (a) Ojima, I.; Slater, J. C.; Kuduk, S. D.; Takeuchi, C. S.; Gimi, R. H.; Sun, C.-M.; Park, Y. H.; Pera, P.; Veith, J. M.; Bernacki, R. J. *Syntheses and Structure–Activity Relationships of Taxoids Derived from 14 β -Hydroxy-10-deacetylbaecatin III*. *J. Med. Chem.* **1997**, *40*, 267–278. (b) Nicoletti, M. L.; Colombo, T.; Rossi,

- C.; Monardo, C.; Stura, S.; Zucchetti, M.; Riva, A.; Morazzoni, P.; Donati, M. B.; Bombardelli, E.; D'Incalzi, M.; Giavazzi, R. IDN5109, a Taxane with Oral bioavailability and Potent Antitumor Activity. *Cancer Res.* **2000**, *60*, 842–846.
- (6) (a) Epothilones (Bollag, D. M.; McQueney, P. A.; Zhu, J.; Hensens, O.; Koupal, L.; Liesch, J.; Goetz, M.; Lazarides, E.; Woods, C. M. Epothilones, a New Class of Microtubule-Stabilizing Agents with a Taxol-Like Mechanism of Action. *Cancer Res.* **1995**, *55*, 2325–2333). (b) Discodermolide (ter Haar, E.; Kowalski, R. J.; Hamel, E.; Lin, C. M.; Longley, R. E.; Gunasekera, S. P.; Rosenkranz, H. S.; Day, B. W. Discodermolide, a Cytotoxic marine Agent that Stabilizes Microtubules more Potently than Taxol. *Biochemistry* **1996**, *35*, 243–250). (c) Eleuthesides (Lindel, T.; Jensen, P. R.; Fenical, W.; Long, B. H.; Casazza, A. M.; Carboni, J.; Fairchild, C. R. Eleutherobin, a New Cytotoxin that Mimics Paclitaxel (Taxol) by Stabilizing Microtubules. *J. Am. Chem. Soc.* **1997**, *119*, 8744–8745). (d) Rhazinilam (Dupont, C.; Guénard, D.; Tchertanov, L.; Thoret, S.; Guéritte, F. D-Ring Substituted Rhazinilam Analogues: Semisynthesis and Evaluation of Antitubulin Activity. *Bioorg. Med. Chem.* **1999**, *7*, 2961–2969). (e) Laulimalides (Mooberry, S. L.; Tien, G.; Hernandez, A. H.; Plubrukarn, A.; Davidson, B. S. Laulimalide and Isolaulimalide, New Paclitaxel-Like Microtubule-Stabilizing Agents. *Cancer Res.* **1999**, *59*, 653–660). (f) WS9885B (Muramatsu, H.; Miyachi, M.; Sato, B.; Yoshimura, S. 40th Symposium on The Chemistry of Natural Products, Fukuoka, Japan, 1998; Paper 83, p 487. See also: Vanderwal, C. D.; Vosburg, D. A.; Weiler, S.; Sorensen, E. J. Postulated Biogenesis of WS9885B and Progress toward an Enantioselective Synthesis. *Org. Lett.* **1999**, *1*, 645–648). (g) Polyisoprenylated benzophenones (Roux, D.; Hadi, H. A.; Thoret, S.; Guénard, D.; Thoison, O.; Païs, M.; Sévenet, T. Structure–Activity Relationship of Polyisoprenyl Benzophenones from *Garcynia pyrifera* on the tubulin/Microtubule System. *J. Nat. Prod.* **2000**, *63*, 1070–1076).
- (7) (a) Winkler, J. D.; Axelsen, P. H. A Model for the Taxol (Paclitaxel)/Epothilone Pharmacophore. *Bioorg. Med. Chem. Lett.* **1996**, *6*, 2963–2966. (b) Wang, M.; Xia, X.; Kim, Y.; Hwang, D.; Jansen, J. M.; Botta, M.; Liotta, D. C.; Snyder, J. P. A Unified and Quantitative Receptor Model for the Microtubule Binding of Paclitaxel and Epothilone. *Org. Lett.* **1999**, *1*, 43–46. (c) Ojima, I.; Chakravarty, S.; Inoue, T.; Lin, S.; He, L.; Horwitz, S. B.; Kuduk, S. D.; Danishefsky, S. J. A Common Pharmacophore for Cytotoxic Natural Products that Stabilize Microtubules. *Proc. Natl. Acad. Sci. U.S.A.* **1999**, *96*, 4256–4261. (d) Giannakakou, P.; Gussio, R.; Nogales, E.; Downing, K. H.; Zaharevitz, D.; Bollbuck, B.; Poy, G.; Sackett, D.; Nicolaou, K. C.; Fojo, T. A Common Pharmacophore for Epothilone and Taxanes: Molecular Basis for Drug Resistance Conferred by Tubulin Mutations in Human Cancer Cells. *Proc. Natl. Acad. Sci.* **2000**, *97*, 2904–2909. (e) He, L.; Jagtap, P. G.; Kingston, D. G. I.; Shen, H.-J.; Orr, G. A.; Horwitz, S. B. A Common Pharmacophore for Taxol and the Epothilones Based on the Biological Activity of a Taxane Molecule lacking a C-13 Side Chain. *Biochemistry* **2000**, *39*, 3972–3978.
- (8) Rodi, D. J.; Janes, R. W.; Sanganee, H. J.; Holton, R. A.; Wallace, B. A.; Makowski, L. Screening of a Library of Phage-Displayed Peptides Identifies Human bcl-2 as a Taxol-binding Protein. *J. Mol. Biol.* **1999**, *285*, 197–203.
- (9) This was first observed by Kingston (Samaranayake, G.; Magri, N. F.; Jitransri, C.; Kingston, D. G. I. Modified Taxols. 5. Reaction of Taxol with Electrophilic Reagents and Preparation of a Rearranged Taxol Derivative with Tubulin Assembly Activity. *J. Org. Chem.* **1991**, *56*, 5114–5119. See also: Chordia, M. D.; Kingston, D. G. I.; Hamel, E.; Lin, C. M.; Long, B. H.; Fairchild, C. A.; Johnston, K. A.; Rose, W. C. Synthesis and Biological Activity of A-nor-Paclitaxel Analogues. *Bioorg. Med. Chem.* **1997**, *5*, 941–947). A partial separation of the tubulin mechanism from the cytotoxic activity has been achieved with some totally synthetic 15(11–12)abeo-2,11-cyclo-2,11-epoxy C-aromatic taxoids derived from borneol (Klar, U.; Graf, H.; Schenk, O.; Röhr, B.; Schulz, H. New Synthetic Inhibitors of Microtubule Depolymerization. *Bioorg. Med. Chem. Lett.* **1998**, *8*, 1397–1402). Among the biological analogues of Taxol, also rhazinilam and the polyisoprenyl benzophenones xanthochymol and guttiferone E show poor cytotoxicity (see refs 6d,g, respectively).
- (10) For leading studies in the area, see: (a) Dubois, J.; Guénard, D.; Guéritte-Voegelein, F.; Guedira, N.; Potier, P.; Gillet, B.; Beloeil, J. C. Conformation of Taxotere and Analogues Determined by NMR Spectroscopy and Molecular Modelling Studies. *Tetrahedron* **1993**, *49*, 6533–6544. (b) Williams, H. J.; Scott, A. I.; Dieden, R. A.; Swindell, C. S.; Chirlian, L. E.; Francl, M. M.; Heerding, J. M.; Krauss, N. E. NMR and Molecular Modelling Study of the Conformation of Taxol and its Side Chain Methyl Ester in Aqueous and Non-Aqueous Solution. *Tetrahedron* **1993**, *49*, 6545–6560. (c) Vander Velde, D. G.; Georg, G. I.; Grunewald, G. L.; Gunn, C. D.; Mitscher, L. A. "Hydrophobic Collapse" of Taxol and Taxotere Solution Conformations in Mixtures of Water and Organic Solvent. *J. Am. Chem. Soc.* **1993**, *115*, 11650–11651. (d) Gomez Paloma, L.; Guy, R. K.; Wrasidlo, W.; Nicolaou, K. C. Conformation of a Water-Soluble Derivative of Taxol in Water by 2D-NMR Spectroscopy. *Chem. Biol.* **1994**, *1*, 107–112. (e) Ojima, I.; Scott, D. K.; Chakravarty, S.; Ourevitch, M.; Bégue, J. P. A Novel Approach to the Study of Solution Structures and Dynamic Behavior of Paclitaxel and Docetaxel Using Fluorine-Containing Analogues as probes. *J. Am. Chem. Soc.* **1997**, *119*, 5519–5527. (f) Milanese, M.; Ugliengo, P.; Viterbo, D.; Appendino, G. Ab Initio Conformational Study of the Phenylisoserine Side Chain of Paclitaxel. *J. Med. Chem.* **1999**, *42*, 291–299. (g) Li, Y.; Poliks, B.; Cegelski, L.; Poliks, M.; Gryczynski, Z.; Piszczek, G.; Jagtap, P. G.; Studelska, D. R.; Kingston, D. G. I.; Schaefer, J.; Bane, S. Conformation of Microtubule-Bound Paclitaxel Determined by Fluorescence Spectroscopy and REDOR NMR. *Biochemistry* **2000**, *39*, 281–291. (h) Snyder, J. P.; Nevins, N.; Cicero, D. O.; Jansen, J. The Conformation of Taxol in Chloroform. *J. Am. Chem. Soc.* **2000**, *122*, 724–725. (i) Snyder, J. P.; Nettles, J. H.; Cornett, B.; Downing, K. H.; Nogales, E. *Proc. Natl. Acad. Sci. U.S.A.*, in press.
- (11) As pointed out in ref 10h, there appear to be three conformational extremes with respect to the orientation of the C13 side chain of Taxol. The polar and apolar forms correspond to hydrophobic collapse between the C2 benzoyl phenyl and the C3' phenyl and C2' benzamide rings, respectively. We refer to the third, uncollapsed, family as "extended" or "open" forms. T-Taxol is one of these in which the centroid of the C2 phenyl is nearly equidistant from the centroids of the two terminal phenyl rings emanating for C3'.¹⁰ⁱ
- (12) Ojima, J.; Lin, S.; Inoue, T.; Miller, M. L.; Borella, C. P.; Geng, X.; and John J. Walsh, J. J. Macrocyclic Formation by Ring-Closing Metathesis. Application to the Syntheses of Novel Macrocyclic Taxoids. *J. Am. Chem. Soc.* **2000**, *122*, 5343–5353.
- (13) Barboni, L.; Lambertucci, C.; Ballini, R.; Appendino, G.; Bombardelli, E. Synthesis of a Conformationally Restricted Analogue of Paclitaxel. *Tetrahedron Lett.* **1998**, *39*, 7177–7180.
- (14) (a) Denis, J.-N.; Fkyerat, A.; Gimbert, Y.; Coutterez, C.; Mantellier, P.; Jost, S.; Greene, A. E. Docetaxel (Taxotere) Derivatives: Novel NbCl₃-Based Stereoselective Approach to 2'-Methyl docetaxel. *J. Chem. Soc., Perkin Trans. 1* **1995**, 1811–1815. (b) Kant, J.; Schwartz, W. S.; Fairchild, C.; Gao, Q.; Huang, S.; Long, B. H.; Kadow, J. F.; Langley, D. R.; Farina, V.; Vyas, D. Diastereoselective Addition of Grignard Reagents to Azetidine-2,3-dione: Synthesis of Novel Taxol Analogues. *Tetrahedron Lett.* **1996**, *37*, 6495–6498.
- (15) For a review, see: Kant, J. The Chemistry of the Taxol Side Chain: Synthesis, Modifications and Conformational Studies. In *The Chemistry and Pharmacology of Taxol and its Derivatives*; Farina, V., Ed.; Elsevier: Amsterdam, 1995; pp 255–300.
- (16) Li, G.; Agert, H. H.; Sharpless, K. B. N-Halocarbamate Salts Lead to More Efficient Catalytic Asymmetric Aminohydroxylation. *Angew. Chem., Int. Ed. Engl.* **1996**, *35*, 2813–1817. For an early application of the aminohydroxylation to the synthesis of the Taxol side chain, see: Li, G.; Sharpless, K. B. Catalytic Asymmetric Aminohydroxylation Provides a Short Taxol Side-chain Synthesis. *Acta Chem. Scand.* **1996**, *50*, 649–651. A recent and remarkable one-step synthesis of the isopropyl ester of the Taxol side chain capitalizes on the asymmetric aminohydroxylation (Song, C. E.; Oh, C. R.; Roh, E. J.; Lee, S.; Choi, J. H. One-step Synthesis of Paclitaxel Side-chain Precursor: Benzamide-based Asymmetric Aminohydroxylation of Isopropyl trans-Cinnamate. *Tetrahedron: Asymmetry* **1999**, *10*, 671–674).
- (17) Seeman, J. I.; Chavdarian, C. G.; Secor, H. V. Synthesis of the Enantiomers of Nornicotine. *J. Org. Chem.* **1985**, *50*, 5419–5421.
- (18) Johnson, R. A.; Nidy, E. G.; Dobrowolski, P. J.; Gebhard, I.; Qualls, S. J.; Wicnienski, N. A.; Kelly, R. C. Taxol Chemistry. 7-O-Triflates as Precursors to Olefins and Cyclopropanes. *Tetrahedron Lett.* **1994**, *35*, 7893–7896. See also Upjohn PCT Application WO 9413655, June 23, 1994.
- (19) (a) Denis, J.-N.; Kanazawa, A. M.; Greene, A. E. Taxotere by Esterification with Stereochemically "Wrong" (2S,3S)-Phenylisoserine Derivatives. *Tetrahedron Lett.* **1994**, *35*, 105–108. (b) Park, H.; Hepperle, M.; Boge, T. C.; Himes, R. H.; Georg, G. I. Preparation of Phenolic Paclitaxel Metabolites. *J. Med. Chem.* **1996**, *39*, 2705–2709.
- (20) Kolb, H. C.; VanNieuwenhze, M. S.; Sharpless, K. B. *Chem. Rev.* **1994**, *94*, 2483–2547. For the asymmetric dihydroxylation of compounds related to **3a,b**, see: Nakajima, M.; Tomioka, K.; Koga, K. *Tetrahedron* **1993**, *49*, 10807–10816.
- (21) Hu, Z.; Erhardt, P. W. Utilization of a Benzoyl Migration to Effect an Expedient Synthesis of the Paclitaxel C-13 Side Chain. *Org. Proc. Res. Dev.* **1997**, *1*, 387–390.
- (22) Koskinen, A. M. P.; Karvinen, E. K.; Siirilä, J. P. Enantioselective Synthesis of the Taxol and Taxotere Side Chain. *J. Chem. Soc., Chem. Commun.* **1994**, *21*, 22.

- (23) Guéritte-Voegelein, F.; Guénard, D.; Mangatal, L.; Potier, P.; Guilhem, J.; Cesario, M.; Pascard, C. Structure of a Synthetic Taxol precursor: *N*-tert-Butoxycarbonyl-10-deacetyl-*N*-debenzoyltaxol. *Acta Crystallogr.* **1990**, *C46*, 781–784.
- (24) Mastropaolo, D.; Camerman, A.; Luo, Y.; Brayer, G. D.; Camerman, N. Crystal and Molecular Structure of Paclitaxel (Taxol). *Proc. Natl. Acad. Sci. U.S.A.* **1995**, *92*, 6920–6924.
- (25) Peterson, J. R.; Do, H. D.; Rogers, R. D. X-ray Structure and Crystal Lattice Interactions of the Taxol Side-Chain Methyl Ester. *Pharm. Res.* **1991**, *8*, 908–912.
- (26) Guéritte-Voegelein, F.; Guénard, D.; Lavelle, F.; Le Goff, M.-T.; Mangatal, L.; Potier, P. Relationship Between the Structure of Taxol Analogues and Their Antimitotic Activity. *J. Med. Chem.* **1991**, *34*, 992–998.
- (27) Wang, M.; Cornett, B.; Nettles, J.; Snyder, J. P. Unpublished.
- (28) (a) Cicero, D. O.; Barbato, G.; Bazzo, R. NMR Analysis of Molecular Flexibility in Solution: A New Method for the Study of Complex Distributions of Rapidly Exchanging Conformations. Application to a 13-Residue Peptide with an 8-Residue Loop. *J. Am. Chem. Soc.* **1995**, *117*, 1027–1033. (b) Nevins, N.; Cicero, D.; Snyder, J. P. A Test of the Single-Conformation Hypothesis in the Analysis of NMR Data for Small Polar Molecules: A Force Field Comparison. *J. Org. Chem.* **1999**, *64*, 3979–3986.
- (29) (a) Mohamadi, F.; Richards, N. G. J.; Guida, W. C.; Liscamp, R.; Lipton, M.; Caufield, C.; Chang, G.; Hendrickson, T.; Still, W. C. MacroModel – an integrated software system for modeling organic and bioorganic molecules using molecular mechanics. *J. Comput. Chem.* **1990**, *11*, 440. (b) Still, W. C.; Tempczyk, A.; Hawley, R. C.; Hendrickson, T. Semianalytical Treatment of Solvation for Molecular Mechanics and Dynamics. *J. Am. Chem. Soc.* **1990**, *112*, 6127–6129. (c) cf. <http://www.schrodinger.com/macromodel2.html>.
- (30) Anisotropic shifts of this type are well-documented in taxoids, the most striking example being the negative (–0.21 ppm) (!) chemical shift value of H-6 α observed for Taxine A in CDCl₃ (Barboni, L.; Gariboldi, P.; Appendino, G.; Enriù, R.; Gabetta, B.; Bombardelli, E. New Taxoids from *Taxus baccata* L. *Liebigs Ann.* **1995**, 345–349). Like Taxol, also Taxine A adopts different conformations in polar and apolar media.
- (31) See for instance: Ali, S. M.; Hoemann, M. Z.; Aubé, J.; Mitscher, L. A.; Georg, G. I.; McCall, R.; Jayasinghe, L. R. Novel Cytotoxic 3'-(*tert*-Butyl) 3'-Dephenyl Analogues of Paclitaxel and Docetaxel. *J. Med. Chem.* **1995**, *38*, 3821–3828.
- (32) Boge, T. C.; Wu, Z.-J.; Himes, R. H.; Vander Velde, D. G.; Georg, G. I. Conformationally Restricted Paclitaxel Analogues: Macrocyclic Mimics of the "Hydrophobic Collapse" Conformation. *Bioorg. Med. Chem. Lett.* **1999**, *9*, 3047–3052.
- (33) Mayer, T. U.; Kapoor, T. M.; Haggarty, S. J.; King, R. W.; Schreiber, S. L.; Mitchison, T. J. Small Molecule Inhibitor of Mitotic Spindle Bipolarity Identified in a Phenotype-Based Screen. *Science* **1999**, *286*, 971–974. For a partial description of the structure, see: *Chem. Eng. News* **1999**, July 26, 44–46.
- (34) Miglietta, A.; Bocca, C.; Gadoni, E.; Gabriel, L.; Rampa, A.; Bisi, A.; Valenti, P.; Da Re, P. Interaction of Geiparvarin and Related Compounds with Purified Microtubular Protein. *Anti-Cancer Drug Des.* **1996**, *11*, 35–48.
- (35) (a) Sengupta, S.; Boge, T. C.; Georg, G. I.; Himes, R. H. Interaction of a Fluorescent Paclitaxel Analogue with Tubulin. *Biochemistry* **1995**, *34*, 11889–11894. (b) See ref 31, except that the MCF-7 breast cancer cell line was used in the cytotoxicity assay.
- (36) Brown, D. S.; Marples, B. A.; Smith, P.; Walton, L. Epoxidation with Dioxiranes Derived from 2-Fluoro-2-substituted-1-tetralones and -1-Indanones. *Tetrahedron* **1995**, *51*, 3587–3606.
- (37) Murphy, J. A.; Patterson, C. W. Regioselectivity of Radical-Induced Bond Cleavages in Epoxides. *J. Chem. Soc., Perkin Trans 1* **1993**, 405–410.
- (38) Denis, J.-N.; Greene, A. E.; Guénard, D.; Guéritte-Voegelein, F.; Mangatal, L.; Potier, P. A Highly Efficient Practical Approach to Natural Taxol. *J. Am. Chem. Soc.* **1988**, *110*, 5917–5919.
- (39) Guéritte-Voegelein, F.; Sénilh, V.; David, B.; Guénard, D.; Potier, P. Chemical Studies of 10-Deacetyl Baccatin III. Hemisynthesis of Taxol Derivatives. *Tetrahedron* **1986**, *42*, 4451–4460.
- (40) Chang, G.; Guida, W. C.; Still, W. C. An Internal Coordinate Monte Carlo Method for Searching Conformational Space. *J. Am. Chem. Soc.* **1989**, *111*, 4379–4386.
- (41) Saunders, M.; Houk, K. N.; Wu, Y.-D.; Still, W. C.; Lipton, M.; Chang, G.; Guida, W. C. Conformations of Cycloheptadecane. A Comparison of Methods for Conformational Searching. *J. Am. Chem. Soc.* **1990**, *112*, 1419–1427.

JM001103V